The Abdus Salam
International Centre for Theoretical Physics

United Nations
Educational, Scientific
and Cultural Organization

International Atomic
Energy Agency

World Year of PHYSICS 2005

H4.SMR/1642-5

"IAG-IASPEI Joint Capacity Building Workshop on Deformation Measurements and Understanding Natural Hazards in Developing Countries"

17 – 23 January 2005

Mapping Deformation of the Earthquake Cycle with InSAR

T.Wright

University of Oxford
U.K.

Strada Costiera 11, 34014 Trieste, Italy - Tel. +39 040 2240 111; Fax +39 040 224 163 - sci_info@ictp.it, www.ictp.it

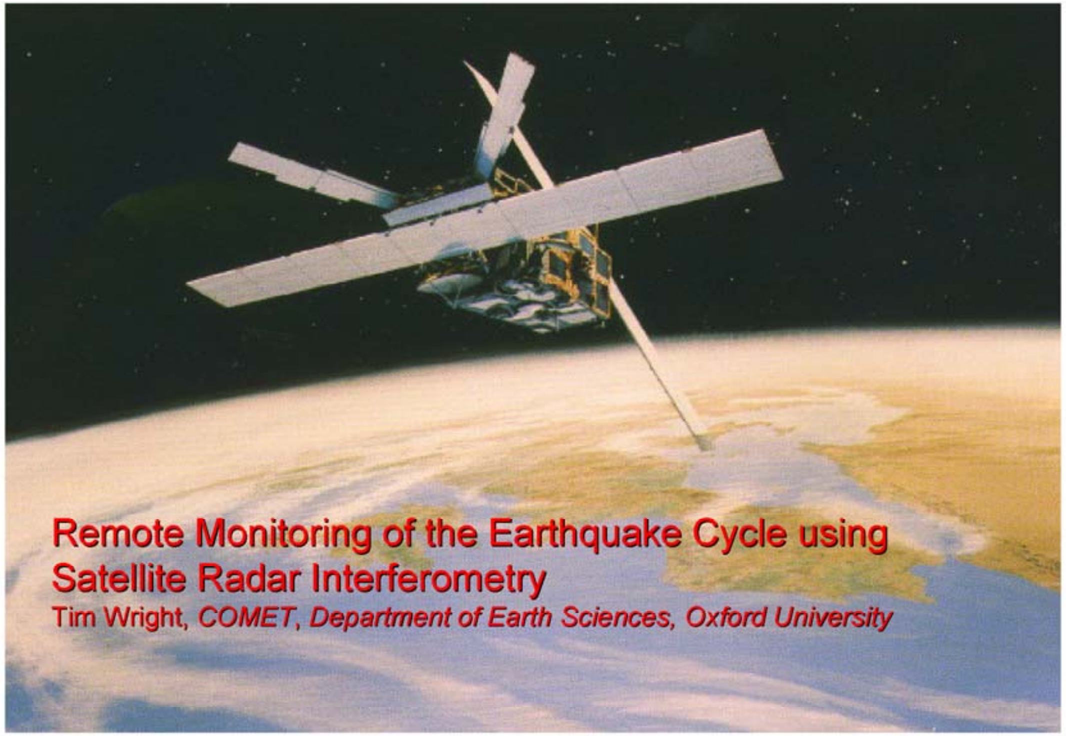

The Earthquake Cycle

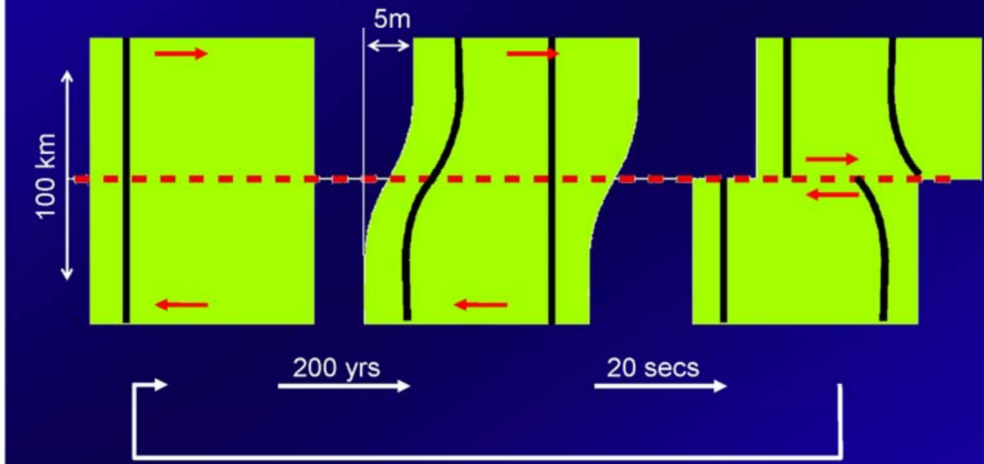

Outline

- The Earthquake Cycle
- Simple elastic dislocation modelling
- Case study: The 2003 Bam earthquake
- Measuring Interseismic deformation with InSAR
- Other EQ cycle phenomena
- Exploiting Envisat and the ERS archive

17 August 1999, Izmit Earthquake

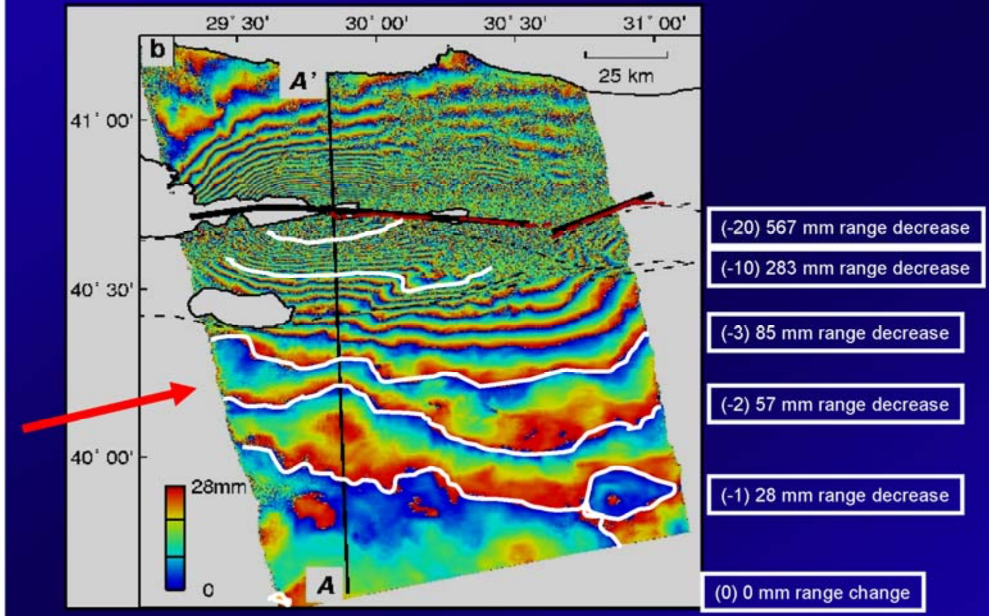

Elastic Dislocation Modelling

OKSAR3 (in today's practical) takes 9 'friendly' fault parameters:

- x, y-position of centre of fault's surface projection in a map projection [2]
- Strike, Dip and Rake of fault (Aki, and Richards convention) [3]
- Magnitude of earthquake slip vector (u_3 = 0, i.e. no opening) [1]
- Top and Bottom Depths (measured vertically), Fault Length [3]

To define a rectangular fault dislocation, need 10 parameters:

- Location of fault x,y,z (x=y=0, z = -d) [1]
- Length, Width and dip of the fault (L, W, δ) [3]
- Slip components (u_1 = strike-slip; u_2 = dip-slip; u_3 = tensile) [3]
- 3D Displacements can be calculated for a point (x_{obs}, y_{obs}) in the fault-centred reference frame, where the x-axis points along strike. [3]

Elastic Dislocation Modelling

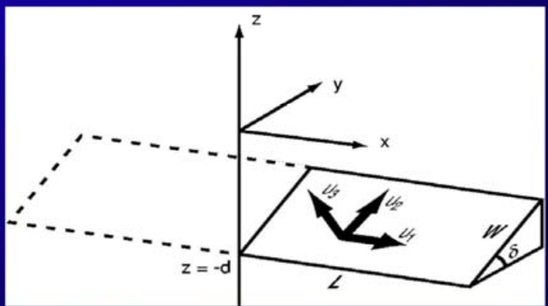

Y. Okada, 1985. Surface deformation due to **shear** and tensile faults in a half-space. *Bull. Seism. Soc. Am.*, 75, 1135-1154

To define a rectangular fault dislocation, need 10 parameters:

- Location of fault x,y,z (x=y=0, z = -d) [1]
- Length, Width and dip of the fault (L, W, δ) [3]
- Slip components (u_1 = strike-slip; u_2 = dip-slip; u_3 = tensile) [3]
- 3D Displacements can be calculated for a point (x_{obs}, y_{obs}) in the fault-centred reference frame, where the x-axis points along strike. [3]

Surface displacements of strike-slip faults

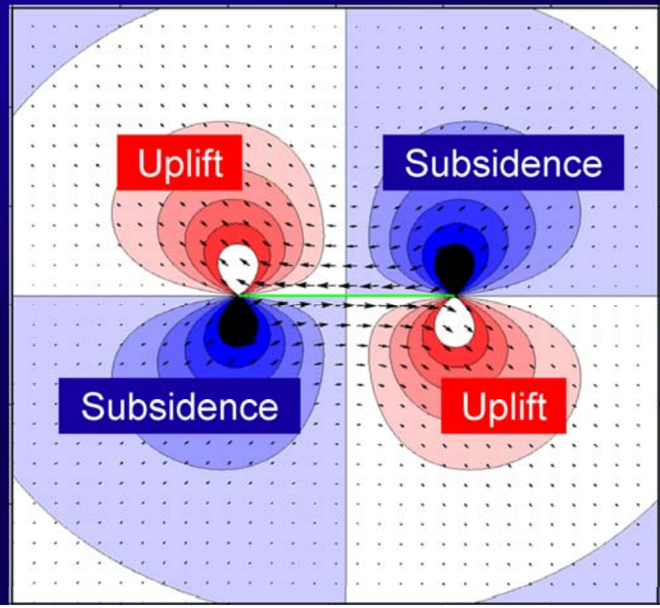

Displacements of normal faults

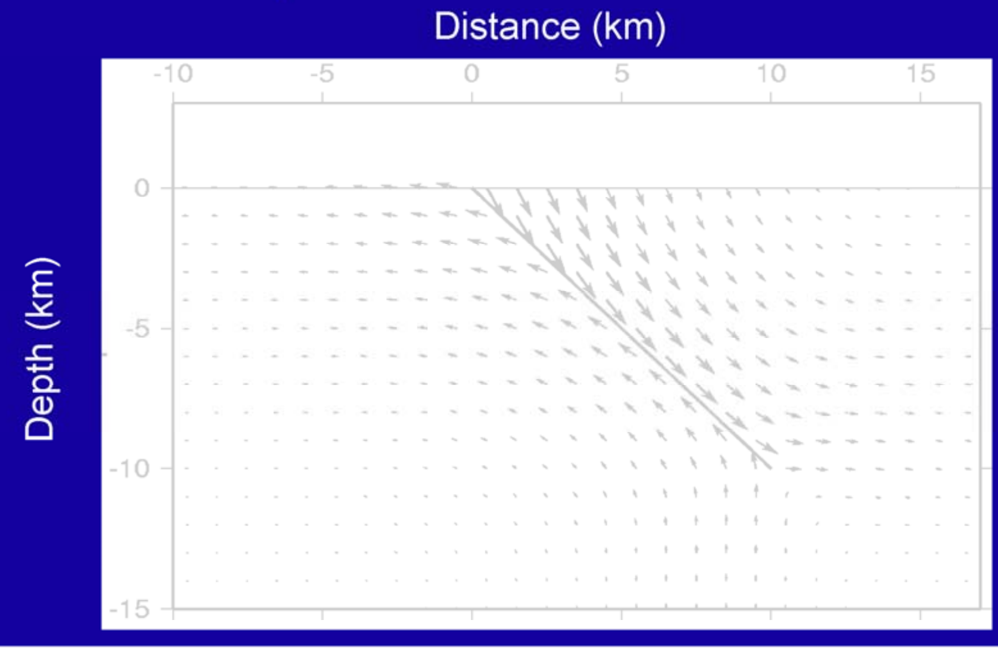

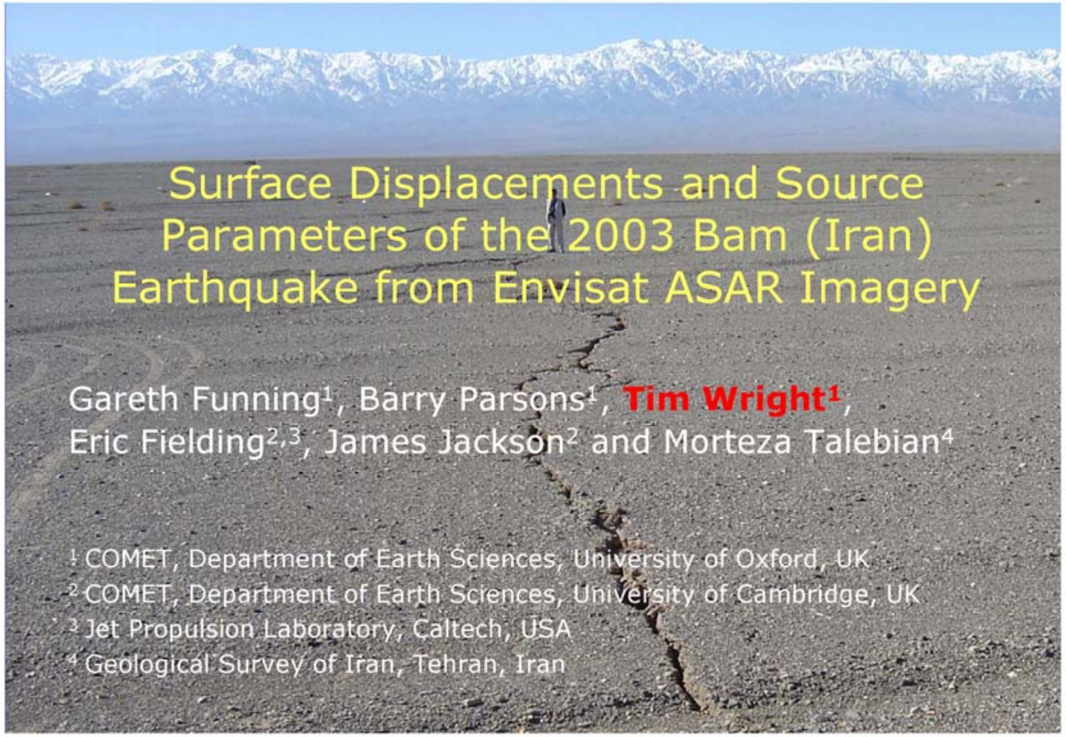

Surface Displacements and Source Parameters of the 2003 Bam (Iran) Earthquake from Envisat ASAR Imagery

Gareth Funning[1], Barry Parsons[1], **Tim Wright[1]**, Eric Fielding[2,3], James Jackson[2] and Morteza Talebian[4]

[1] COMET, Department of Earth Sciences, University of Oxford, UK
[2] COMET, Department of Earth Sciences, University of Cambridge, UK
[3] Jet Propulsion Laboratory, Caltech, USA
[4] Geological Survey of Iran, Tehran, Iran

Determining best-fit elastic models

- Calculating the predicted displacements from a specified fault geometry (forward modelling) is relatively easy.
- The inverse problem (finding the model that fits a given set of displacements) is harder:
  - Finding the fault geometry is a non-linear inversion problem.
  - Determining slip distributions for a fixed fault geometry is a linear problem.

26th December 2003, M_w 6.6

Tectonic setting

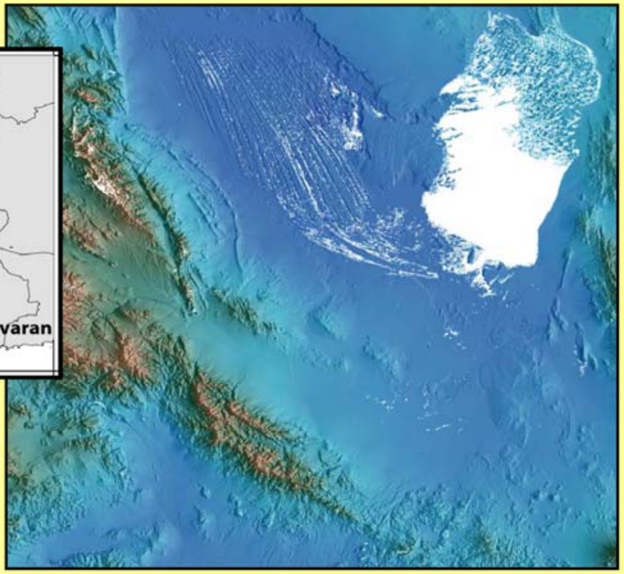

SRTM shaded-relief topography

Tectonic setting

Nayband fault

Gowk fault

Sabzevaran fault

SRTM shaded-relief topography

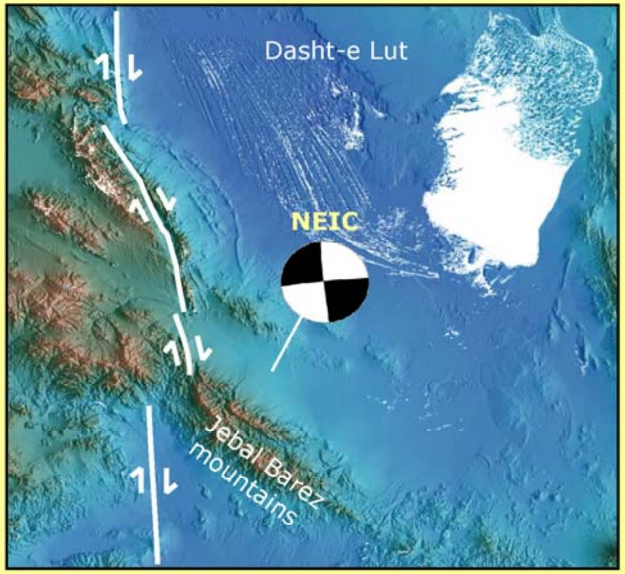

Tectonic setting

Nayband fault

Gowk fault

Sabzevaran fault

SRTM shaded-relief topography

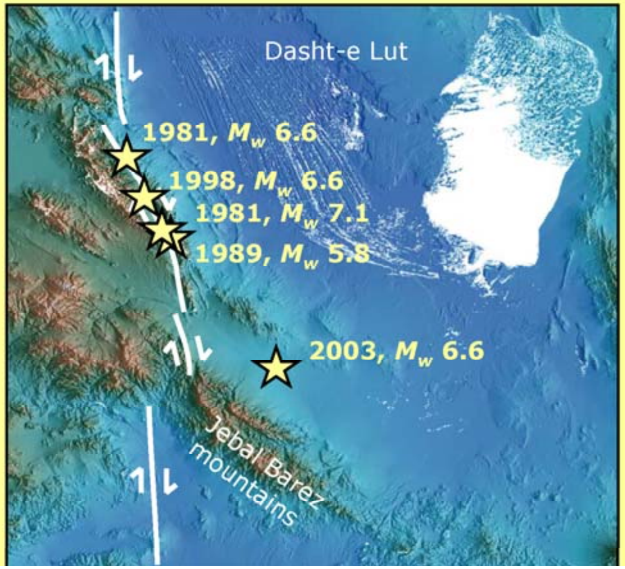

Tectonic setting

Nayband fault

Gowk fault

Sabzevaran fault

SRTM shaded-relief topography

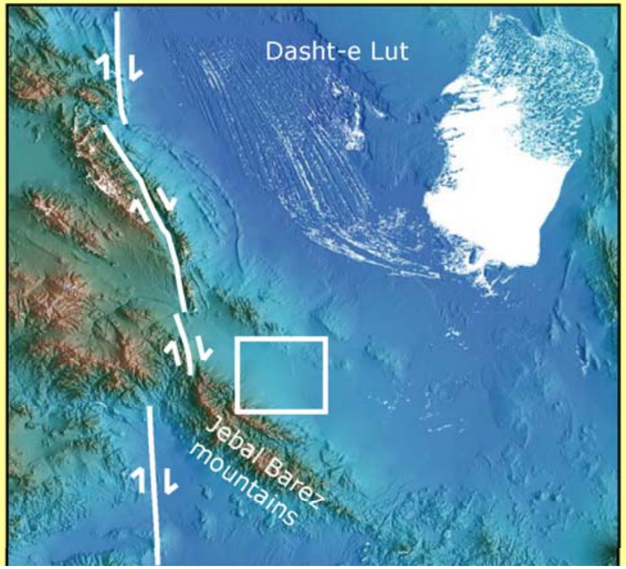

The Bam area

Main geomorphic features of the Bam area:

2: The Bam fault – a prominent ridge running between Bam and Baravat

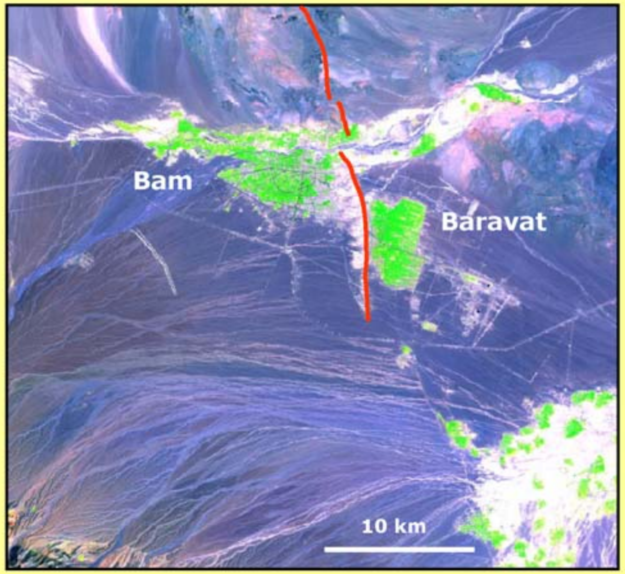

LANDSAT-7 ETM 541 false colour green=vegetation

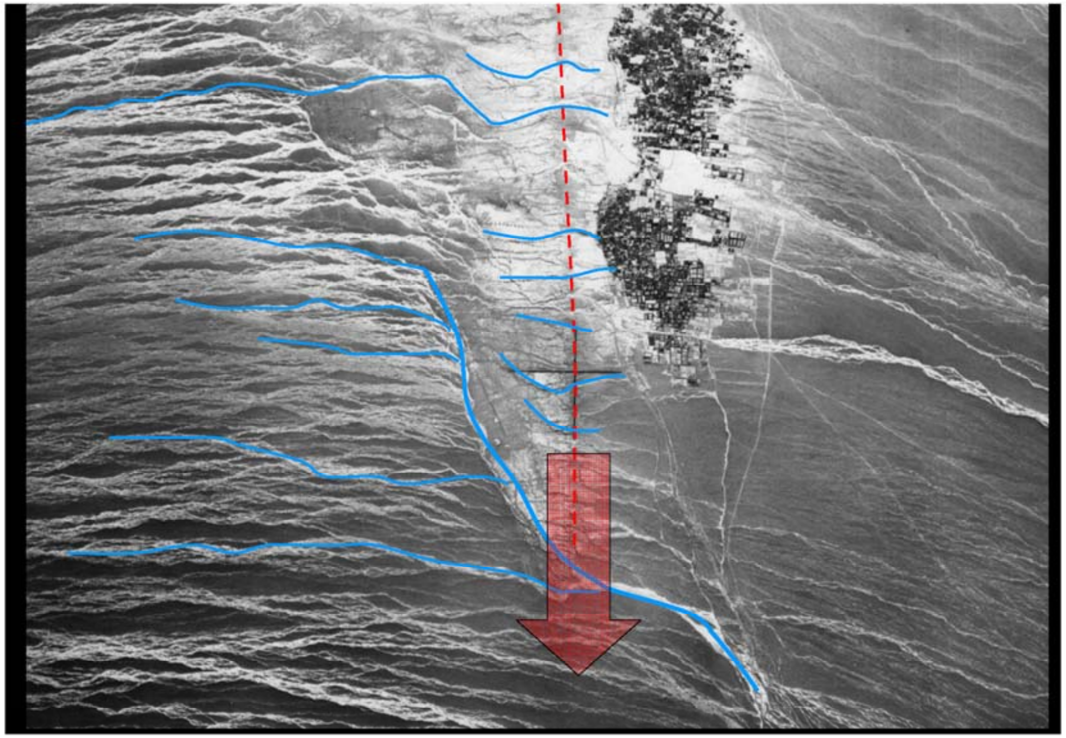

The Bam fault

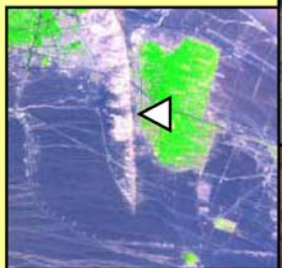

The Bam fault is marked by a 20m-high ridge

The Bam fault

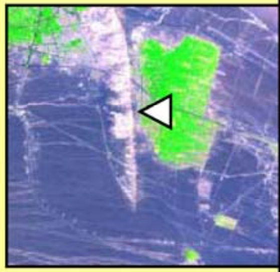

Post-earthquake field surveys found only minor cracking at the foot of the ridge...

The Bam fault

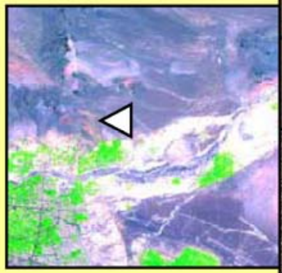

…and fault ruptures observed in the north were also minor
(< 5 cm offset)

Preliminary InSAR data

First Bam interferogram (each colour cycle=2.8cm of deformation)

Constructed from Envisat ASAR data released for free by ESA

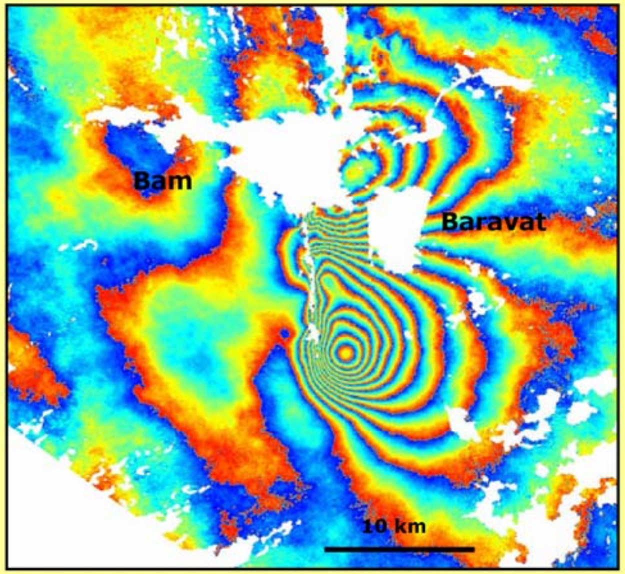

The Bam fault ?

BUT…

More damage in Bam than Baravat

Peak vertical acceleration of ~1g in central Bam

Very small surface rupture on Bam fault

LANDSAT-7 ETM 541 false colour green=vegetation

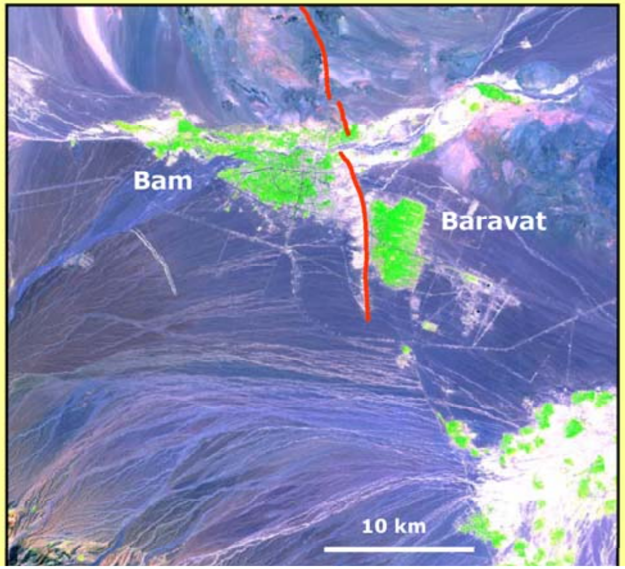

Preliminary InSAR data

There is a prominent band of incoherence running S of Bam

First Bam interferogram (each colour cycle=2.8cm of deformation)

Constructed from Envisat ASAR data released for free by ESA

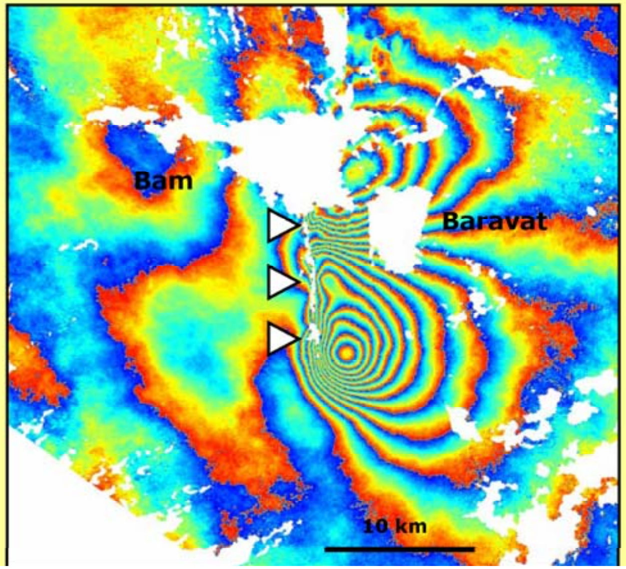

The Bam earthquake main fault

Low coherence indicates vegetation and surface damage

Interferometric coherence
Red = high
Blue = low

Constructed from Envisat ASAR data released for free by ESA

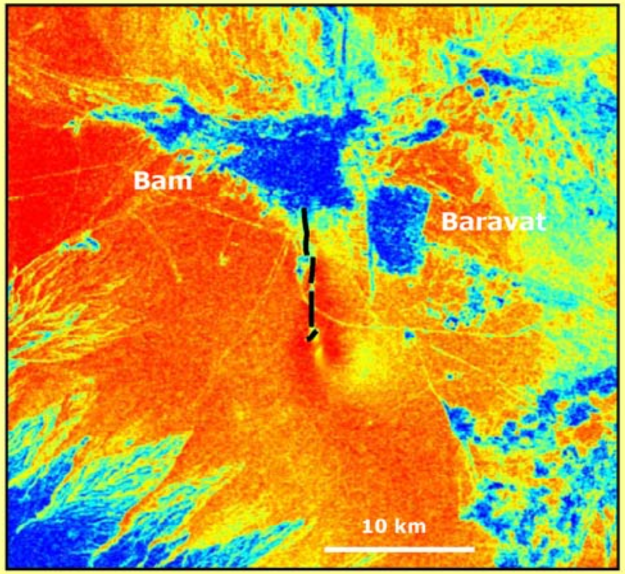

The Bam earthquake main fault

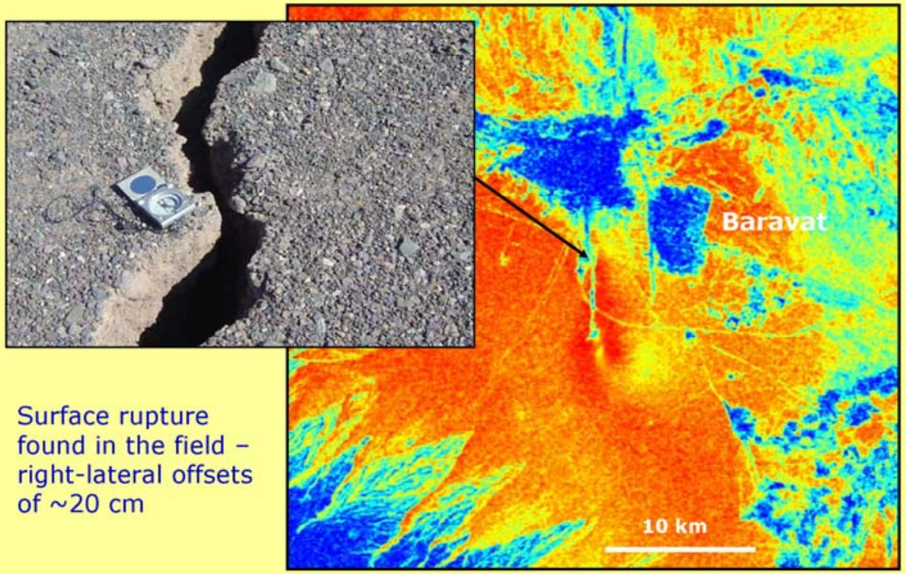

Surface rupture found in the field – right-lateral offsets of ~20 cm

The Bam earthquake main fault

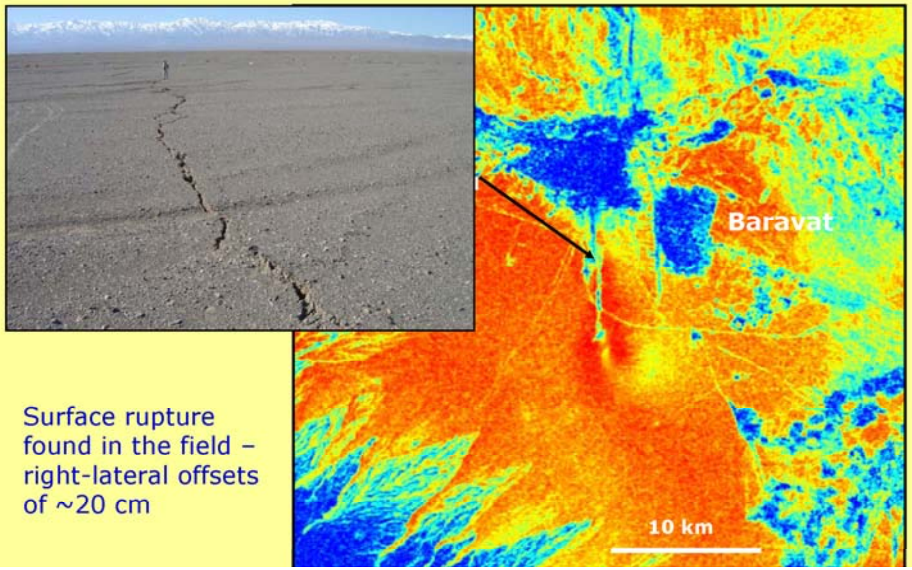

Surface rupture found in the field – right-lateral offsets of ~20 cm

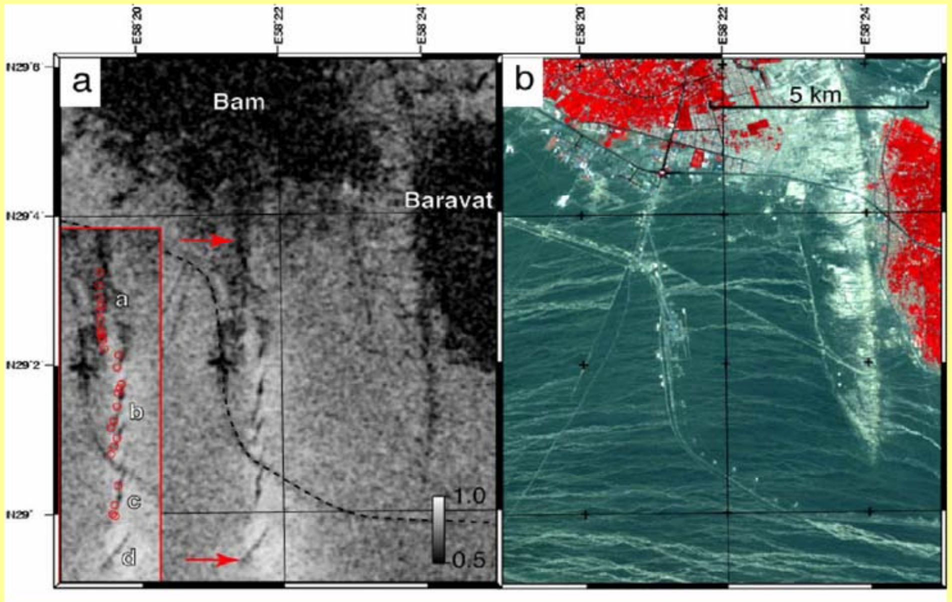

ASAR data for the Bam earthquake

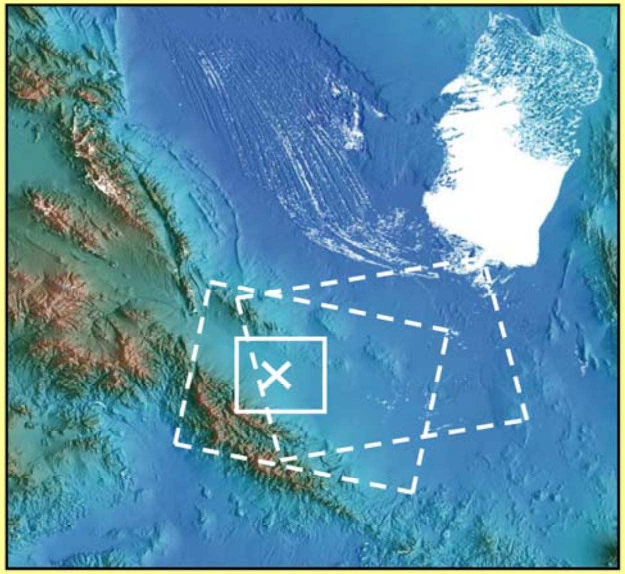

SRTM shaded-relief topography

Ascending track interferogram

Track 385, beam mode I2, 16/11/2003 – 25/01/2004

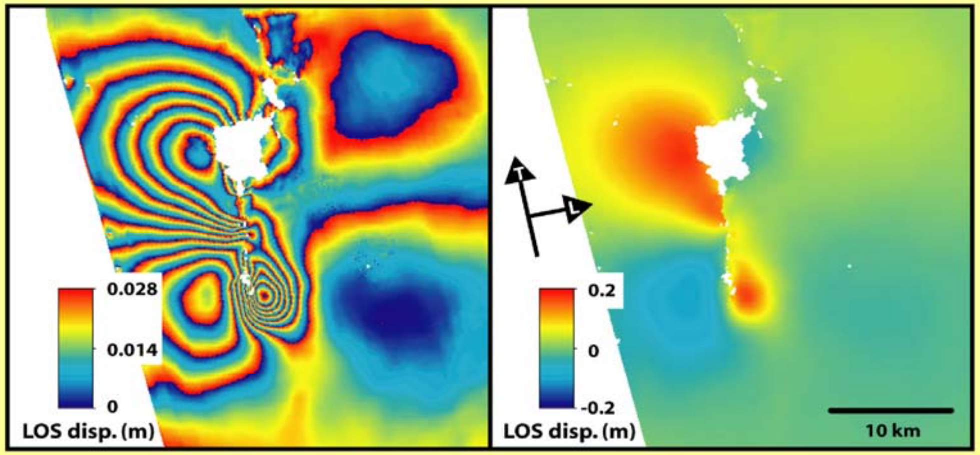

Wrapped

Unwrapped

Descending track interferogram

Track 120, beam mode I2, 03/12/2003 – 07/02/2004

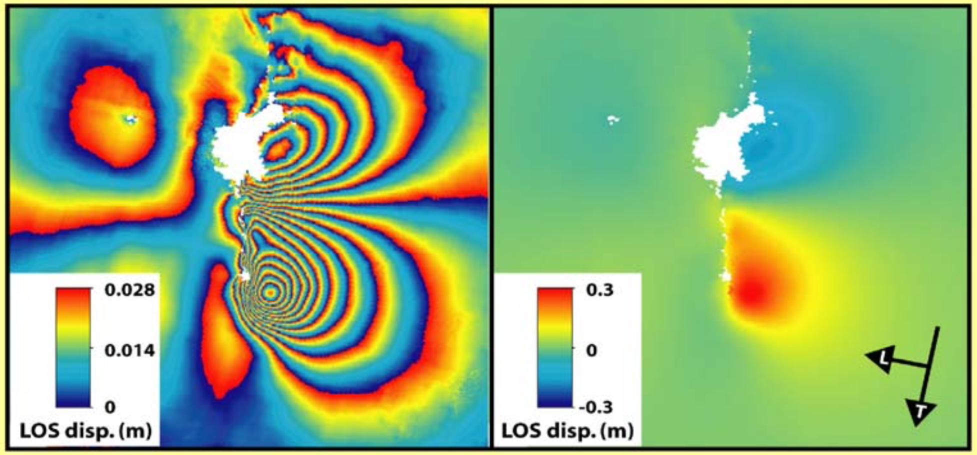

Wrapped

Unwrapped

Azimuth offsets

Ascending

Descending

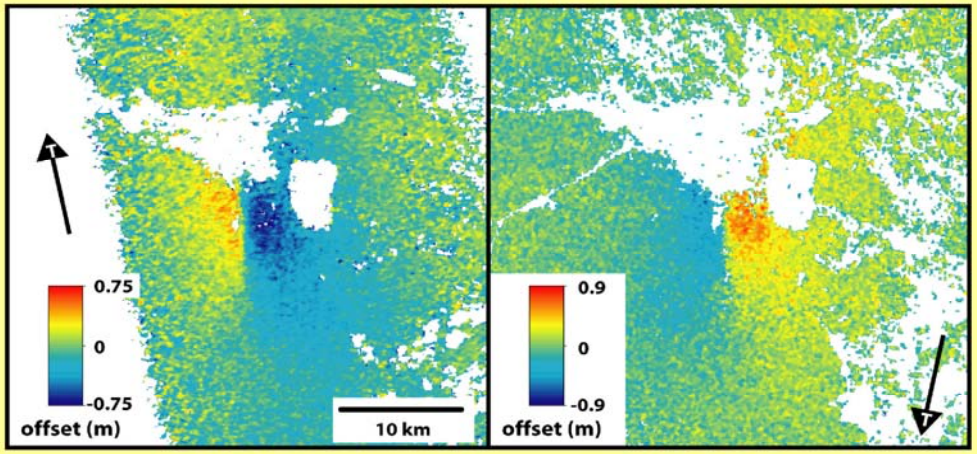

Determining 3D displacements

If the 3D displacement at a pixel is given by $\mathbf{u} = [u_x, u_y, u_z]$, then…

Ascending interferogram, $d_1 = \mathbf{los_A} \bullet \mathbf{u}$

Descending interferogram, $d_2 = \mathbf{los_D} \bullet \mathbf{u}$

Ascending az. offsets, $d_3 = \mathbf{los_{AO}} \bullet \mathbf{u}$

Descending az. offsets, $d_4 = \mathbf{los_{DO}} \bullet \mathbf{u}$

Which can be rewritten as a matrix equation, $\mathbf{d} = \mathbf{Lu}$, and solved for $\mathbf{u}$.

See e.g. Wright, T.J, B. Parsons, Z. Lu., Geophys Res. Lett. 30(18), p.1974, 2003

Bam earthquake 3D displacements

East North Up

Data

Vert. pure s-s

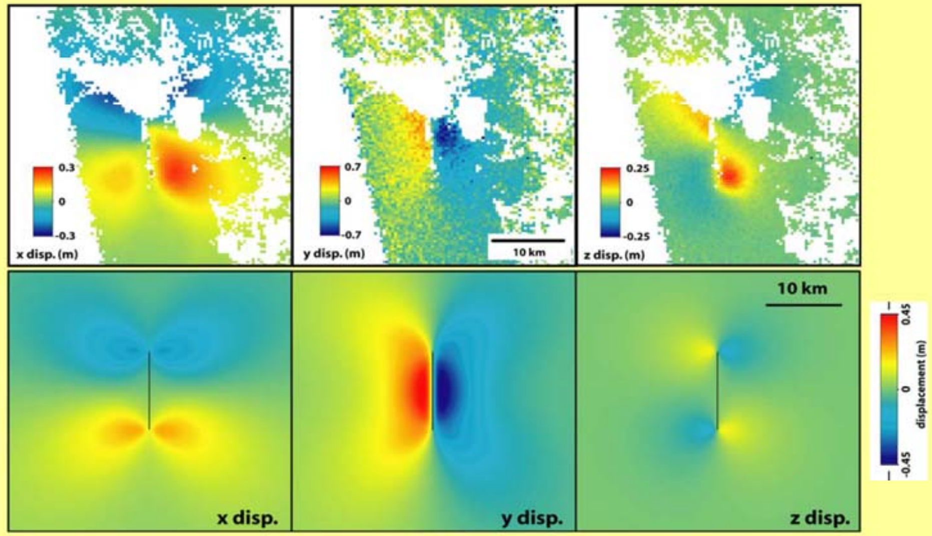

Bam earthquake 3D displacements

East North Up

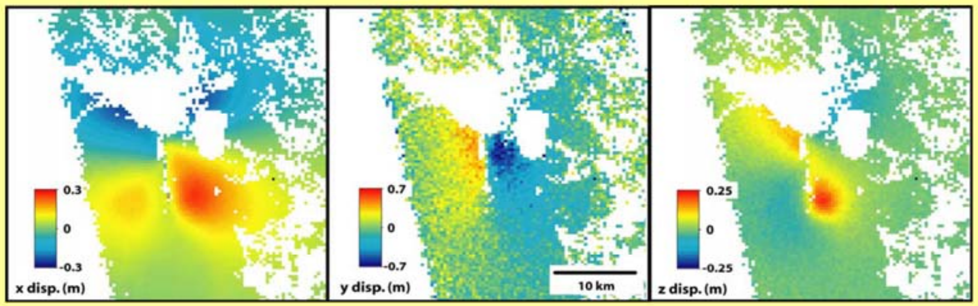

$\sigma = 0.01$ m $\sigma = 0.09$ m $\sigma = 0.01$ m

Single fault, uniform-slip model

Strike 354 dip 84 rake -177 slip 2.2m length 12km top 1.1km b'm 9.3km

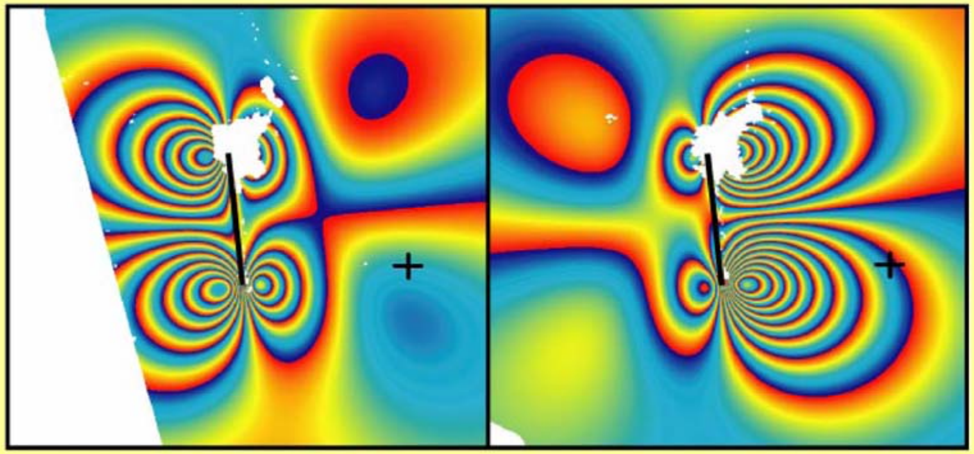

Ascending model Descending model

Single fault model

Large residuals, especially in SE quadrant (rms = 25 mm)

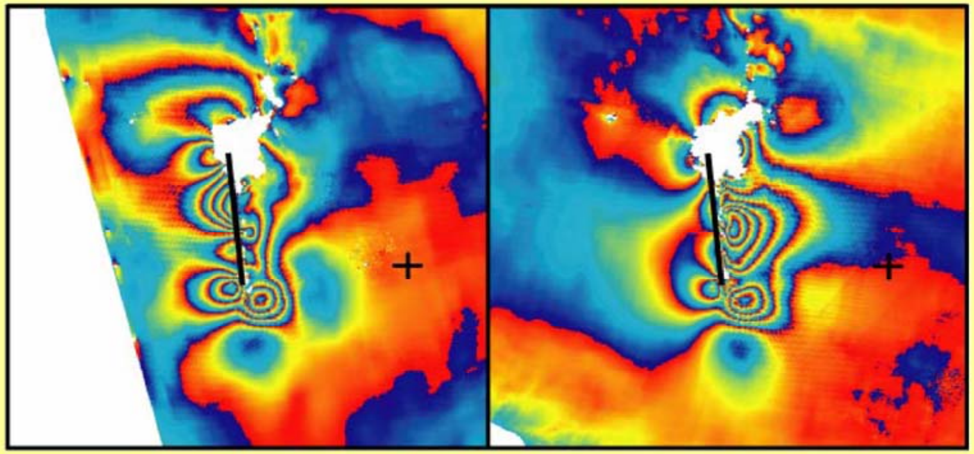

Ascending residual　　　Descending residual

Is it a single fault...?

There is an ‘extra’ amount of displacement in the SE quadrant

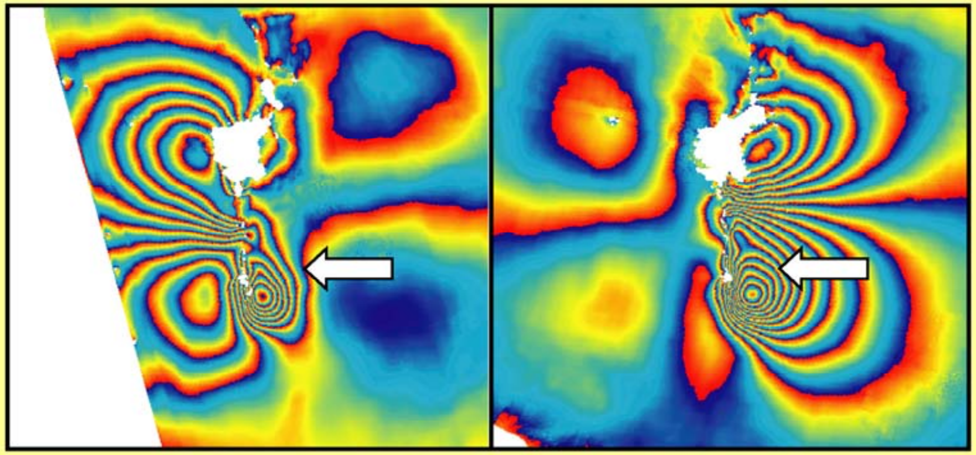

Ascending interferogram　　　Descending interferogram

Bam earthquake 3D displacements

East　North　Up

Data

Vert. pure s-s

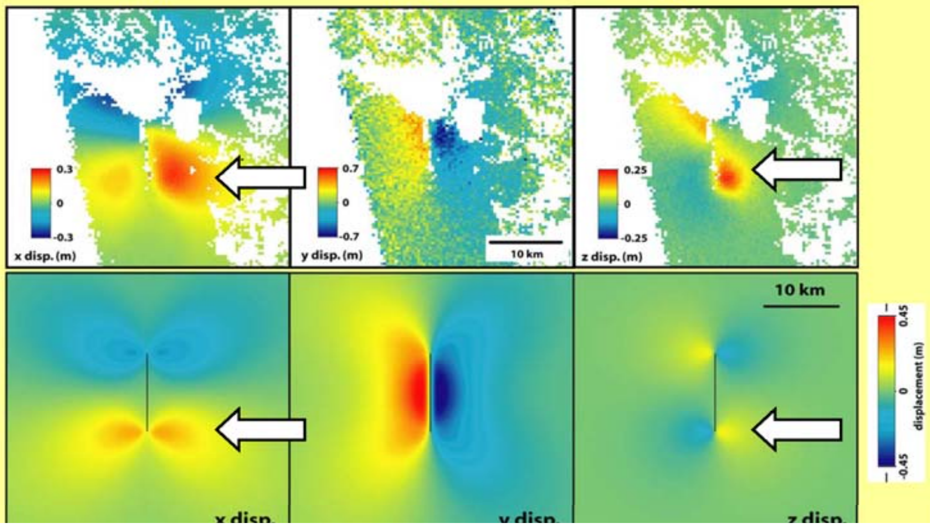

Bam 031226: single source
354/86/182/6/7.6E18

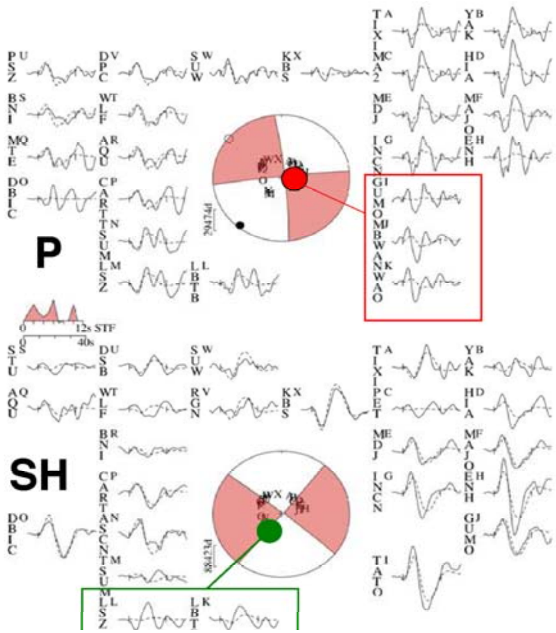

Two fault model

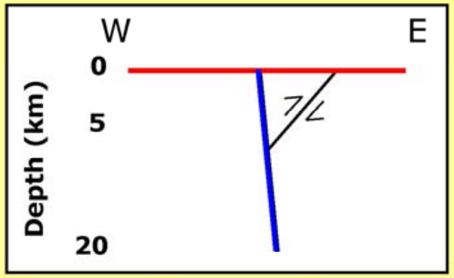

- Main fault: strike 354, dip 85, rake -178, slip 2.1m, length 12km, top 1.2km, bottom 9.8km, M_0 7.6 x 10^{18} Nm

- Secondary fault: strike 180, dip 63, rake 149, slip 1.8m, length 15km, top 6.0km, bottom 7.2km, M_0 1.3 x 10^{18} Nm

Two fault model (uniform slip)

Improved fit in SE quadrant (rms = 17 mm)

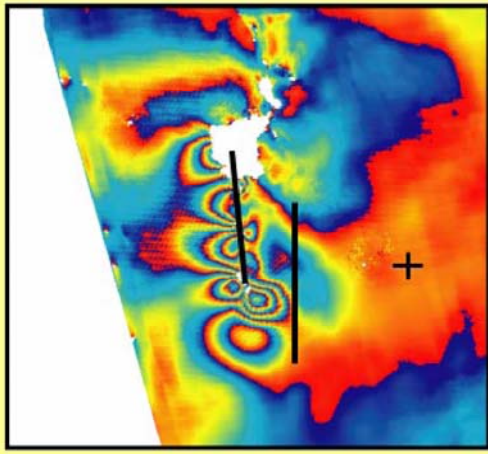

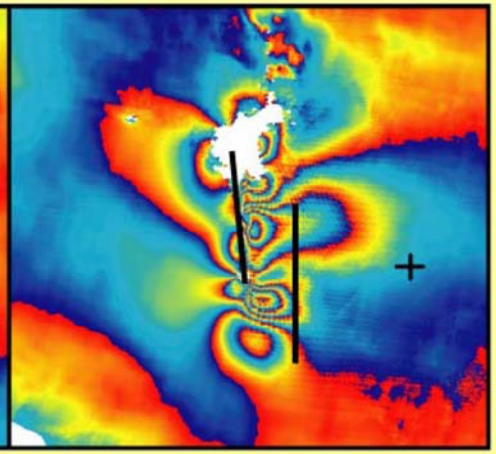

Ascending residual

Descending residual

Two fault model (uniform slip)

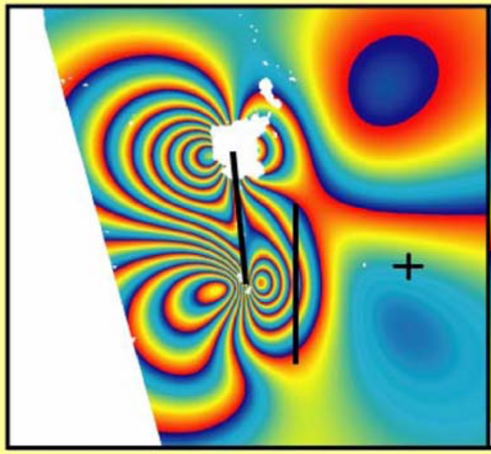

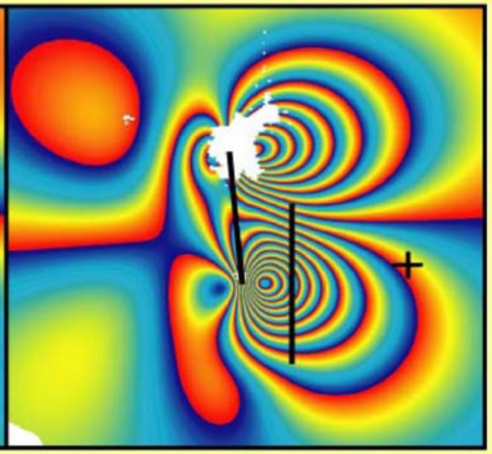

Ascending model

Descending model

Variable slip model

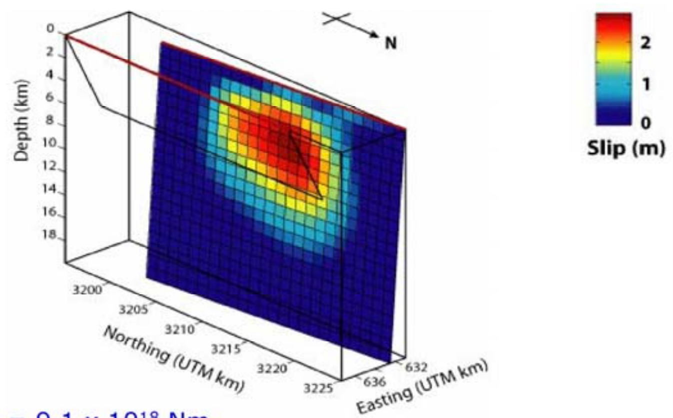

Main fault, M_0 = 9.1 x 10^{18} Nm

Variable slip model

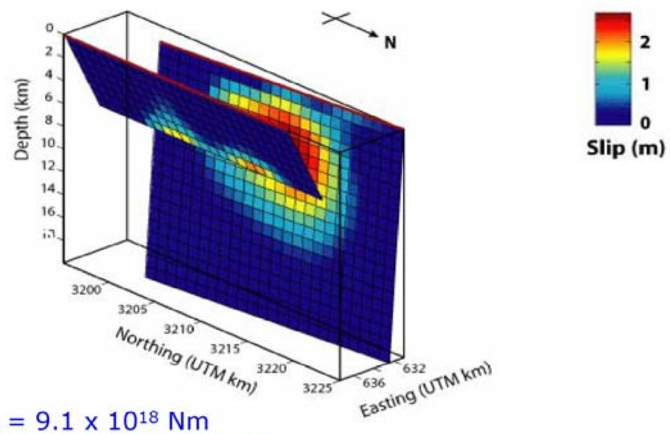

Main fault, M_0 = 9.1 x 10^{18} Nm

Secondary fault, M_0 = 1.6 x 10^{18} Nm

Variable slip model

Significantly improved fit (rms = 13 mm)

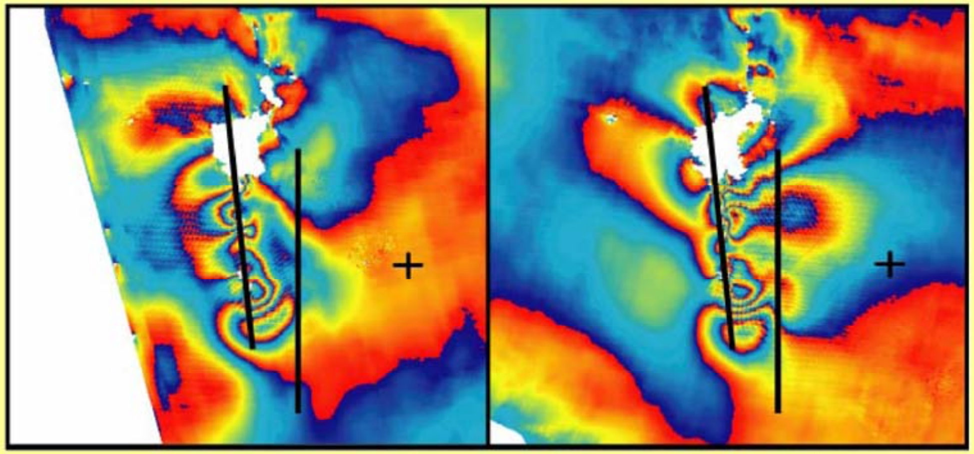

Ascending residual

Descending residual

Variable slip model

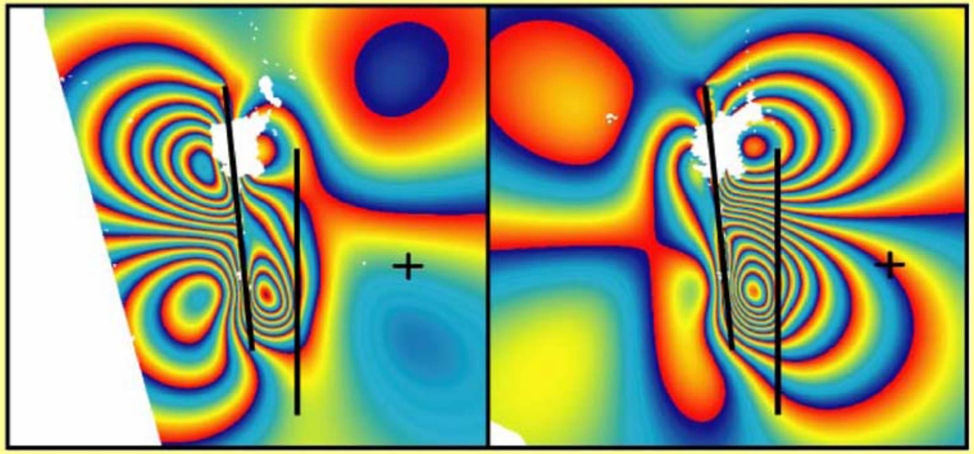

Ascending model

Descending model

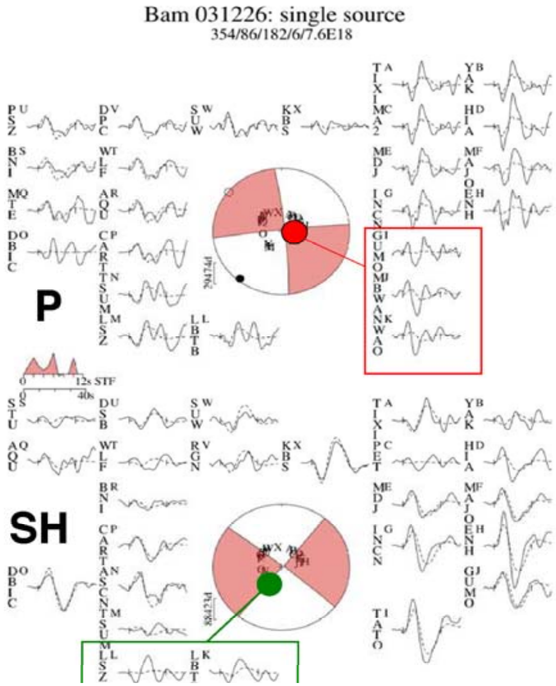

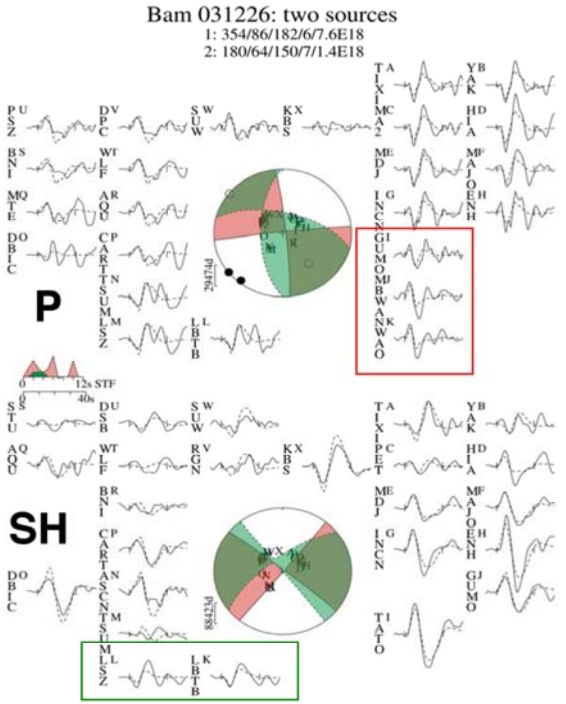

Two fault model

Secondary fault appears to be a southward continuation of the Bam fault

- Geodesy ✓
- Seismology ✓
- Geomorphology ✓

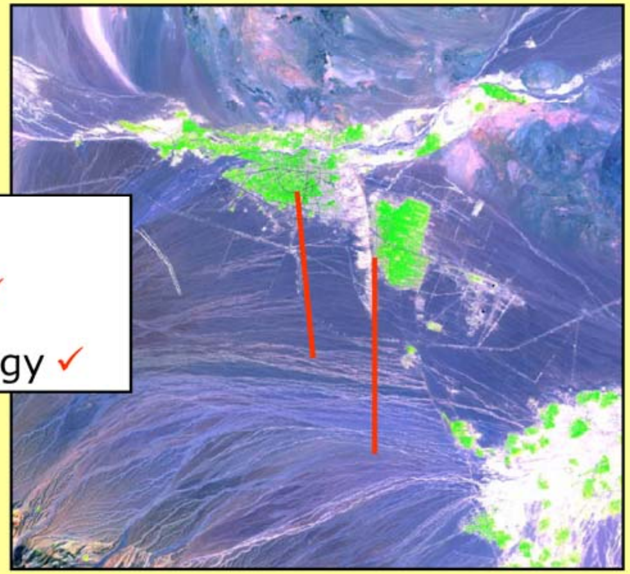

LANDSAT-7 ETM
541 false colour
green=vegetation

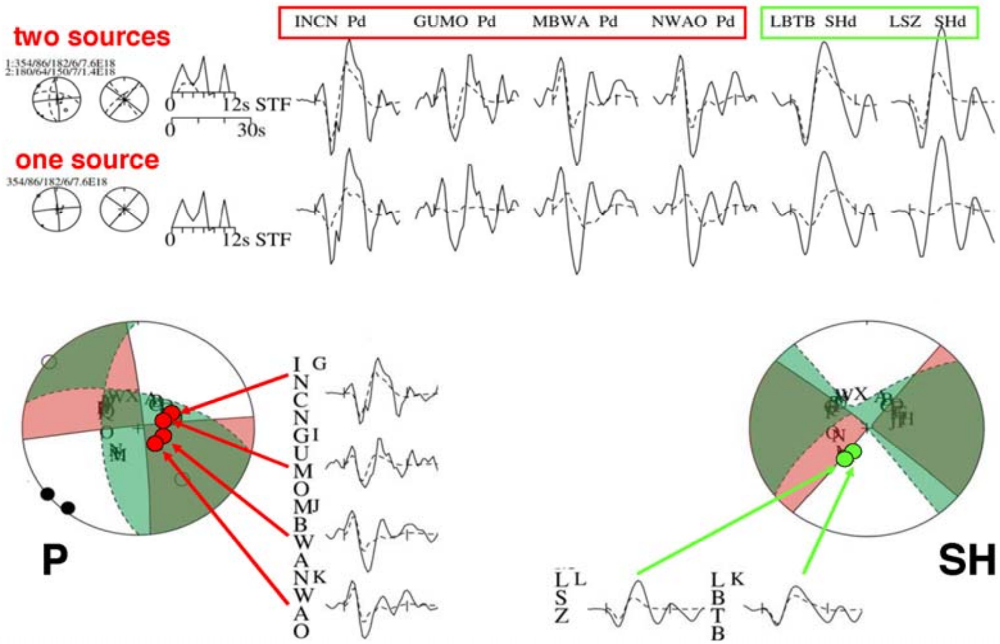

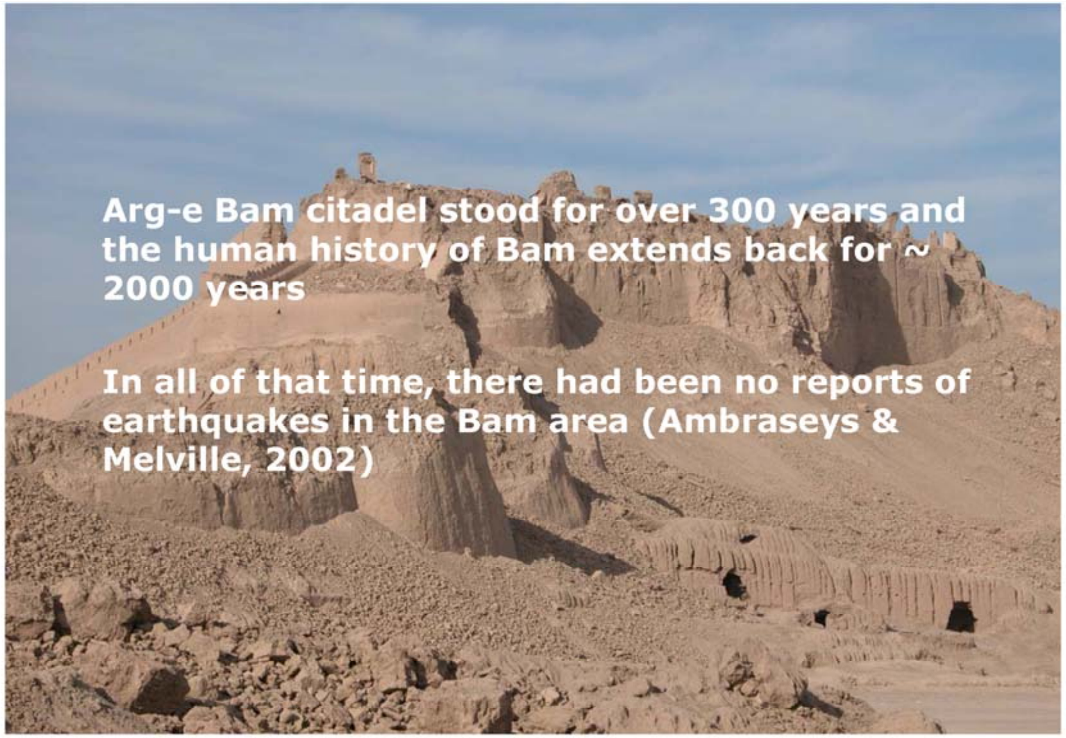
Arg-e Bam citadel stood for over 300 years and the human history of Bam extends back for ~ 2000 years
In all of that time, there had been no reports of earthquakes in the Bam area (Ambraseys & Melville, 2002)

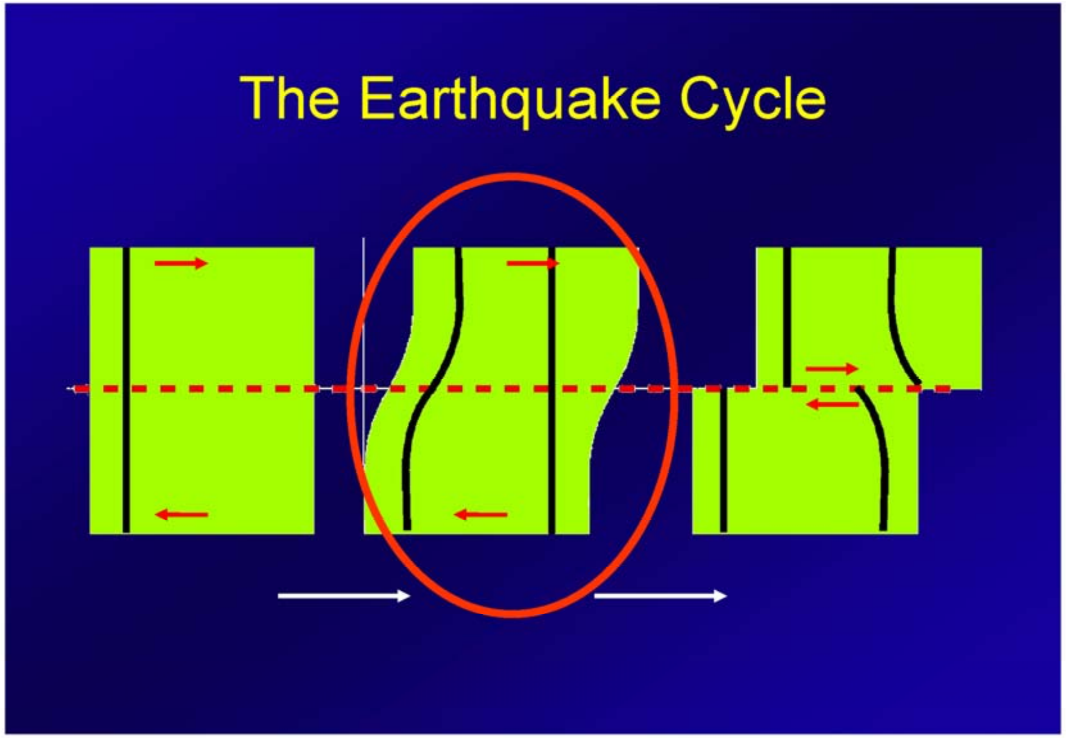
The Earthquake Cycle

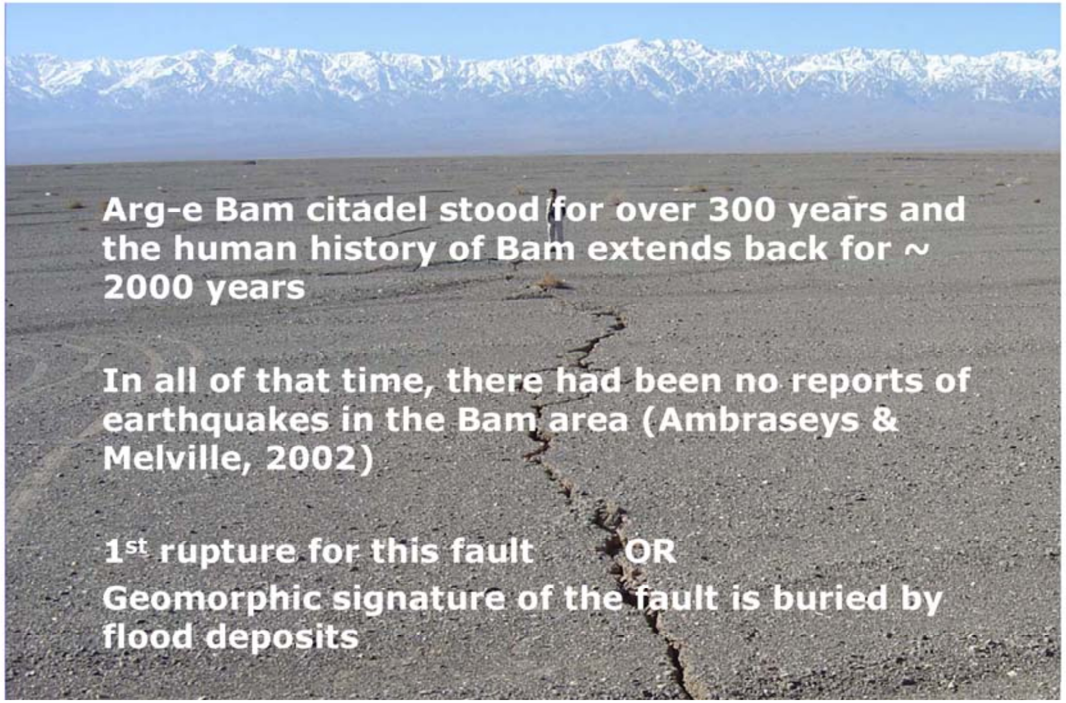
Arg-e Bam citadel stood for over 300 years and the human history of Bam extends back for ~ 2000 years
In all of that time, there had been no reports of earthquakes in the Bam area (Ambraseys & Melville, 2002)
1st rupture for this fault OR
Geomorphic signature of the fault is buried by flood deposits

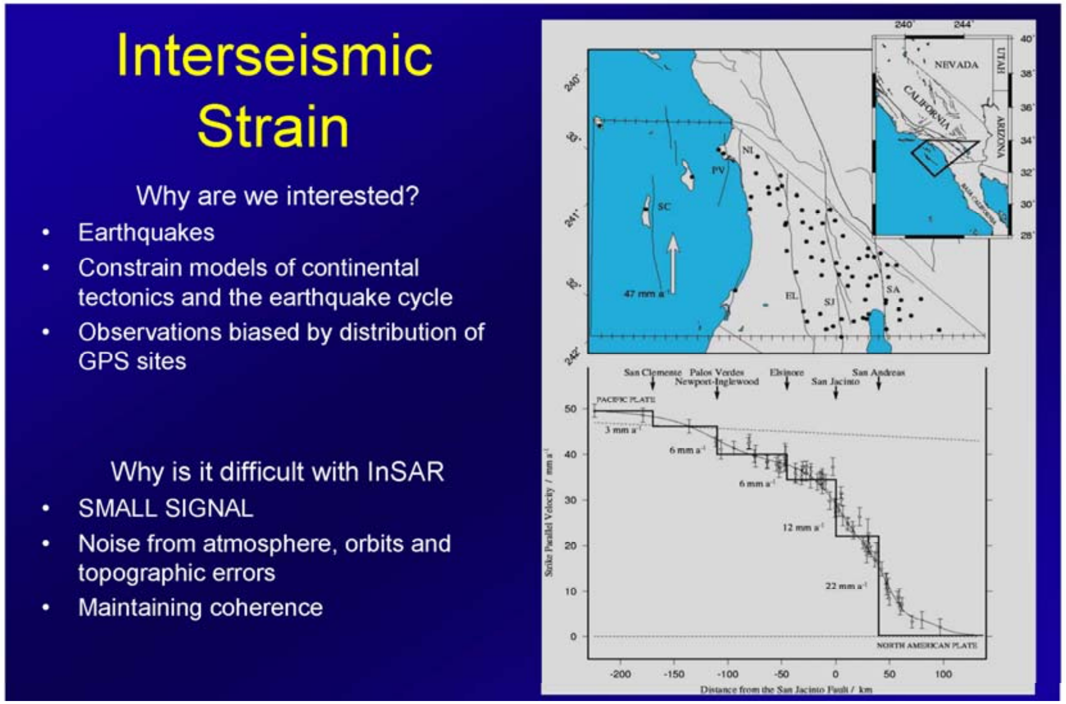
Interseismic Strain
Why are we interested?
• Earthquakes
• Constrain models of continental tectonics and the earthquake cycle
• Observations biased by distribution of GPS sites
Why is it difficult with InSAR
• SMALL SIGNAL
• Noise from atmosphere, orbits and topographic errors
• Maintaining coherence
NEVADA
PACIFIC PLATE
NORTH AMERICAN PLATE
San Clemente
Palos Verdes
Newport-Inglewood
Elsinore
San Jacinto
San Andreas
Distance from the San Jacinto Fault / km

Interseismic Fault creep
– Hayward Fault, California

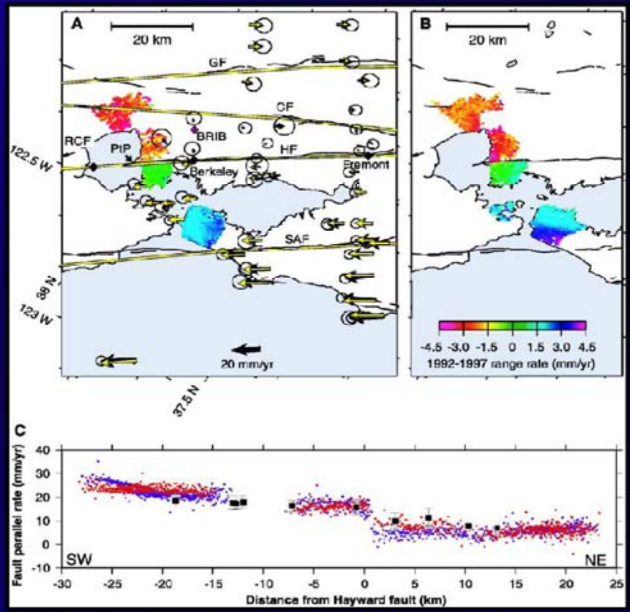

(Burgmann et al, Science, 2000)

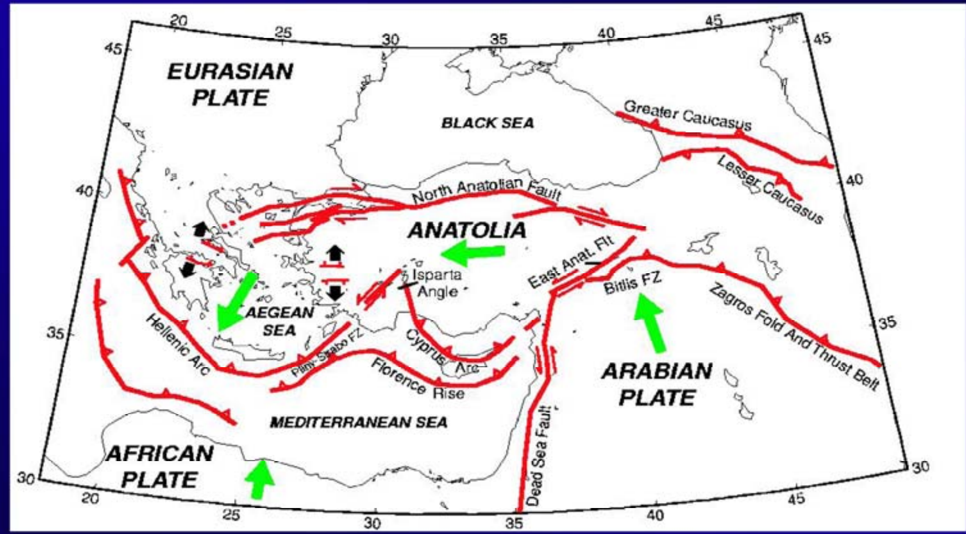

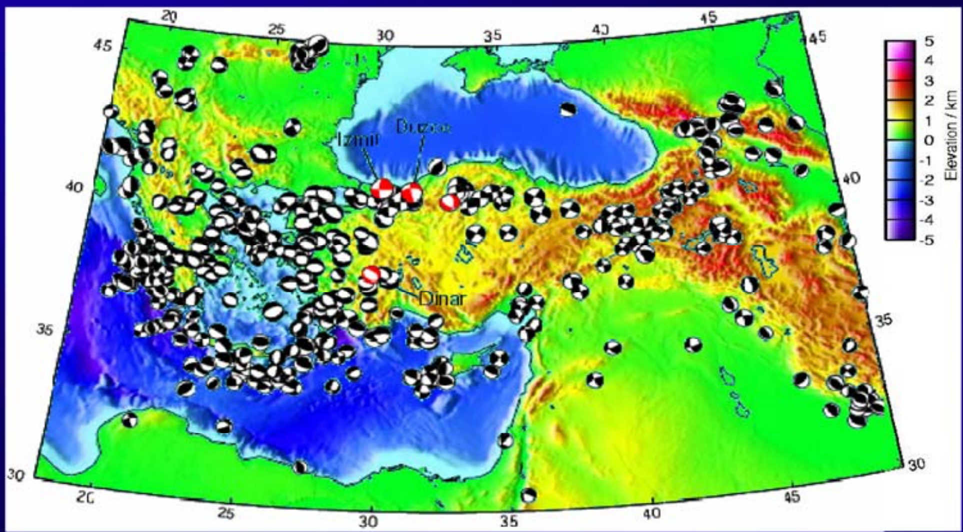

Seismicity: 1894 – 1988 (Most events with $M_w > 6$; Jackson & McKenzie, 1988)
1976 – 2000 (Most events with $M_w > 5$; Harvard CMT)

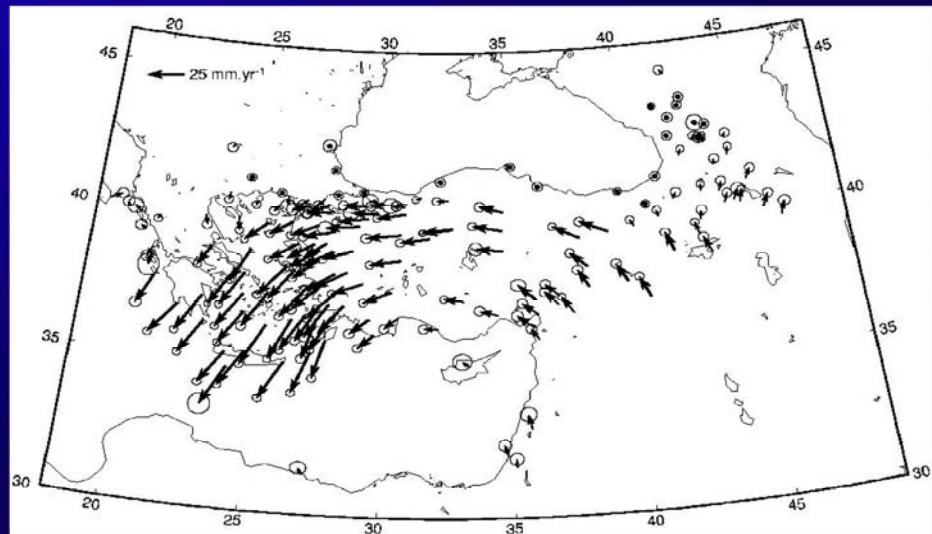

(McClusky et al, JGR, 2000)

The North Anatolian Fault

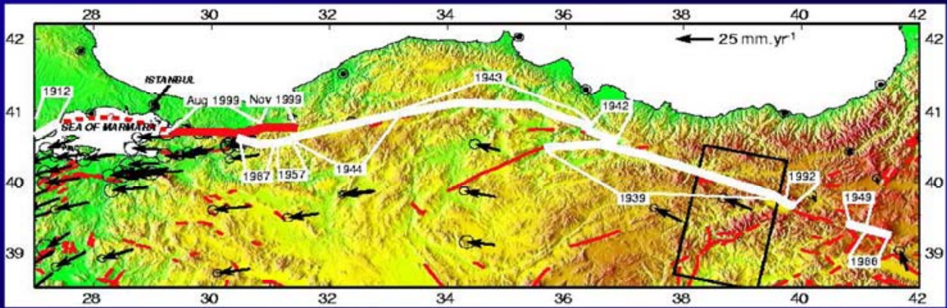

- ~1300 km long
- Slip rate from GPS = 24±1 mm/yr
- 20th Century earthquake sequence
- Single strand in most places
- Good GPS in west, poor in east
- Orientation good for InSAR

Incoherent

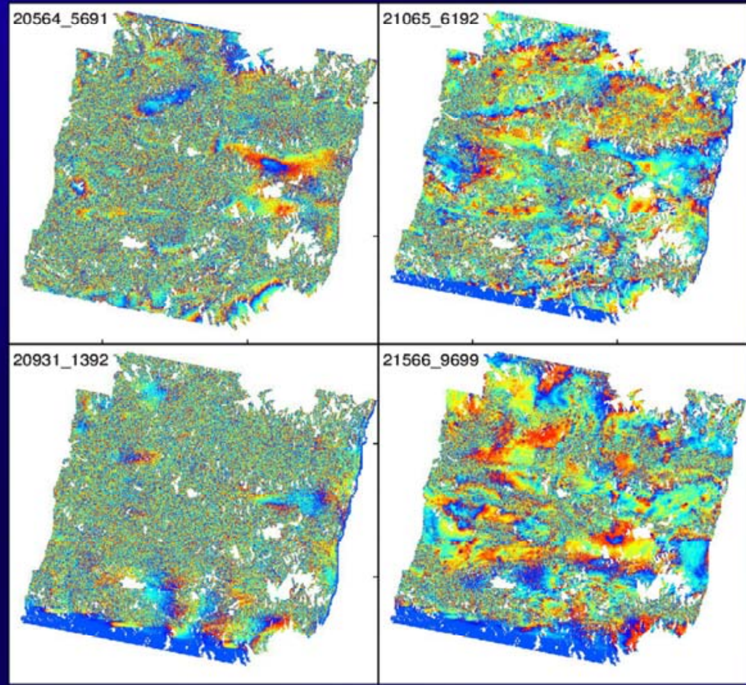

Track 35

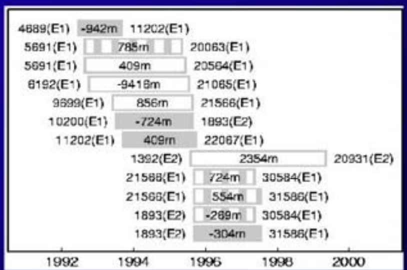

- Processed 12 interferograms
  - 1 yr < Δt < 4 yrs
  - h_a > 250m

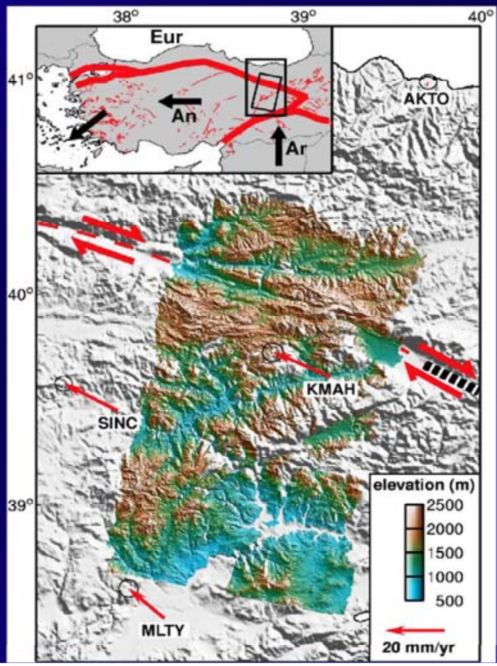

Strong atmospheric signal

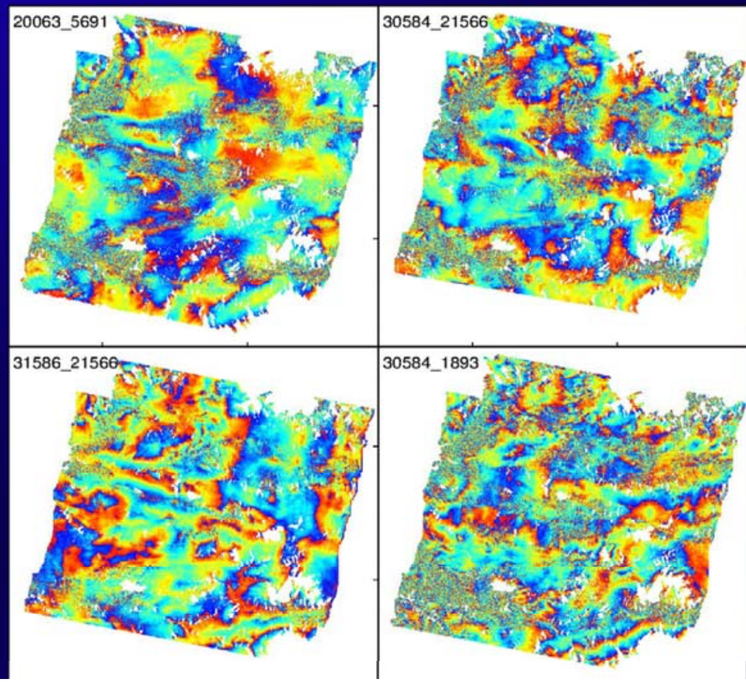

Good

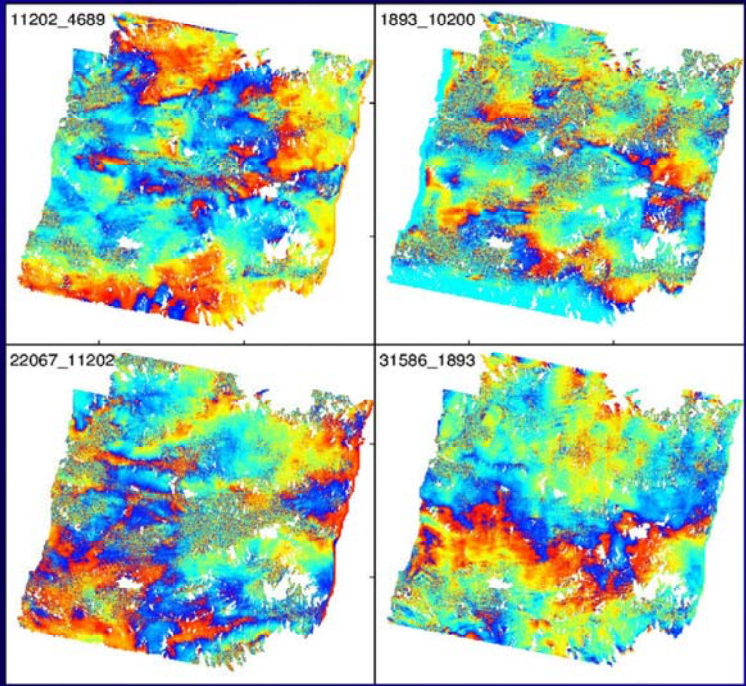

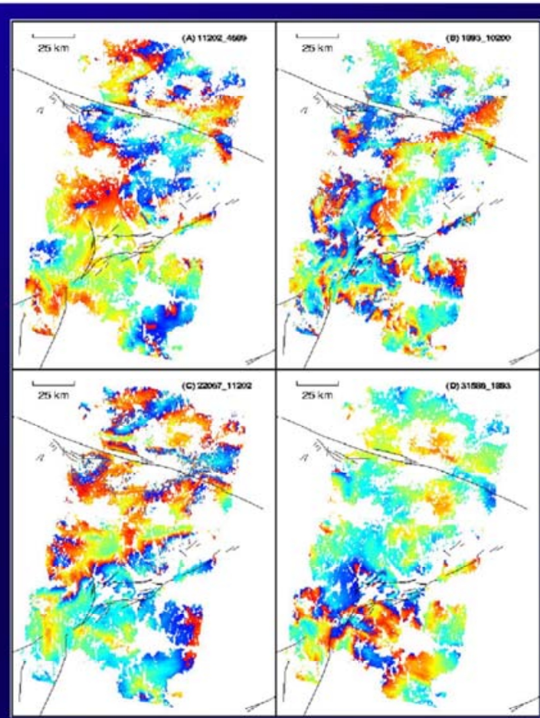

Orbital error ?

- If only have 100 km of data ⇒ ambiguity between orbit error and deformation

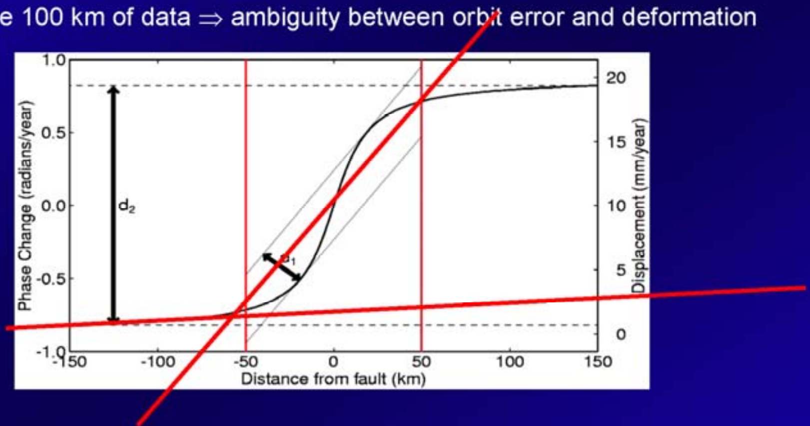

- Extend profile to South ⇒ impossible to fit linear orbital tilt to expected signal

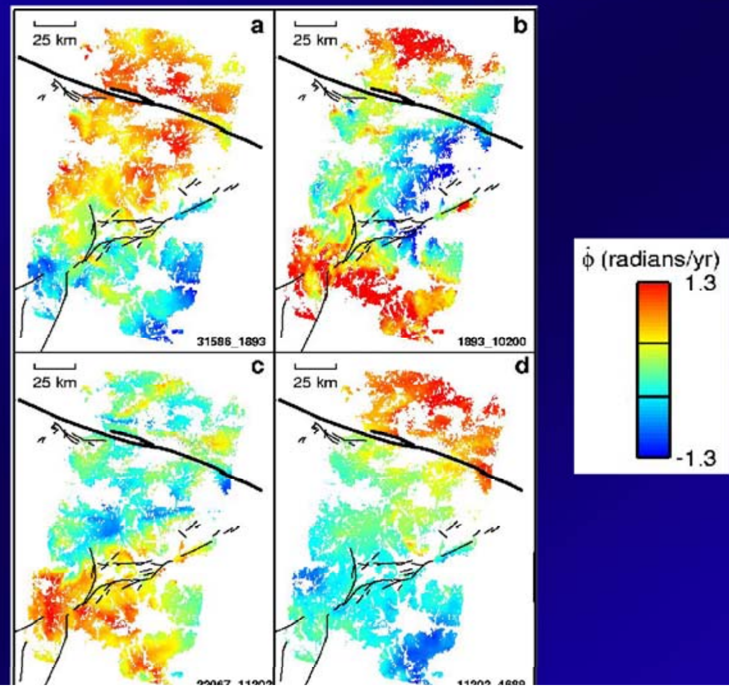

Stack = $\frac{I1 + I2 + I3 + I4}{\Sigma \text{ (time intervals)}}$

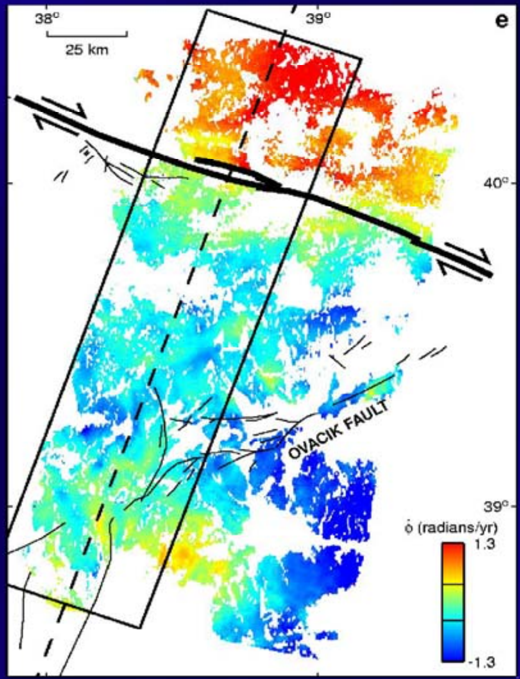

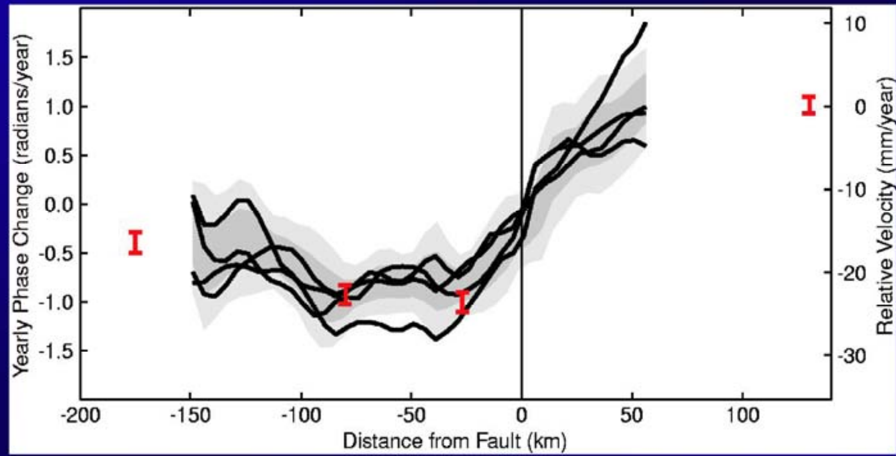

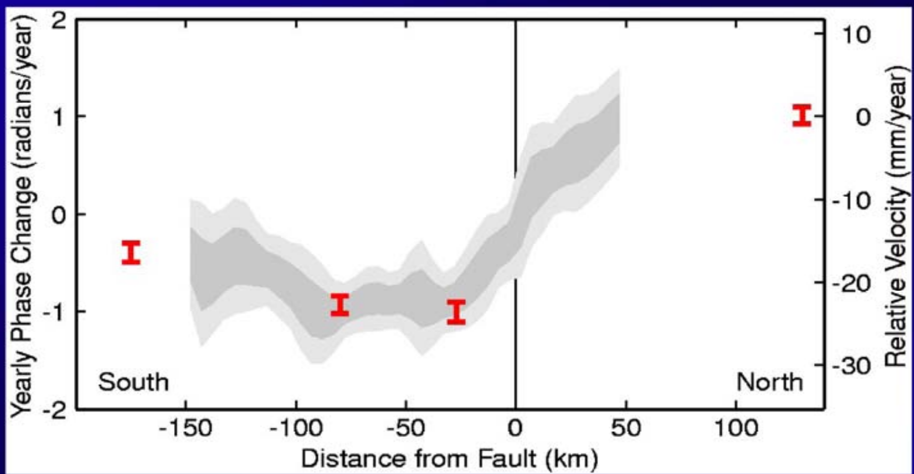

Simple dislocation model

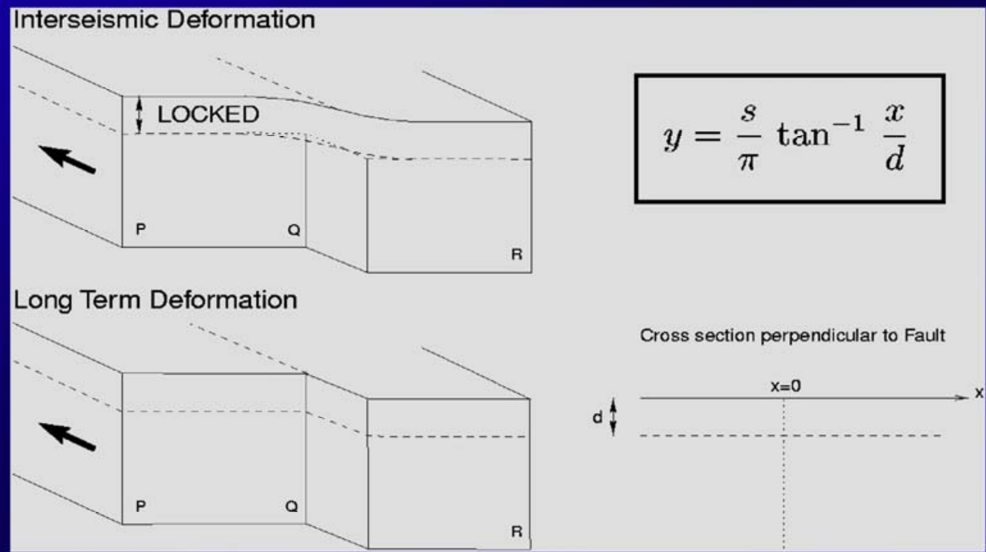

$$y = \frac{s}{\pi} \tan^{-1} \frac{x}{d}$$

Savage & Burford (1973)

Simple dislocation model

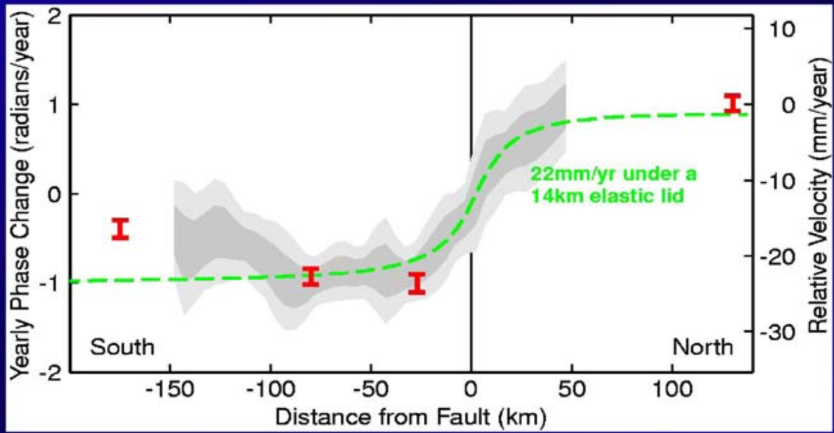

Simple dislocation model

- Determine uncertainties with Monte-Carlo simulation approach
  - Find best fit model to 100 profiles perturbed using the estimated error
  - Range of parameters found ⇒ uncertainties on parameters
  - Strong trade-off between slip and locking depth

- Slip = 17-32 mm/yr
- Locking Depth = 5-33 km
- If GPS slip rate of 24 ± 1 m/yr is correct
  ⇒ locking depth = 18 ± 6 km

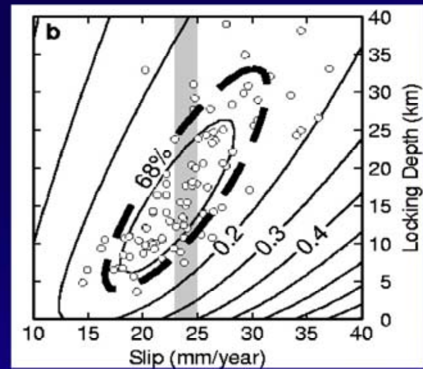

Wright, Parsons and Fielding, GRL 2001

Simple dislocation model

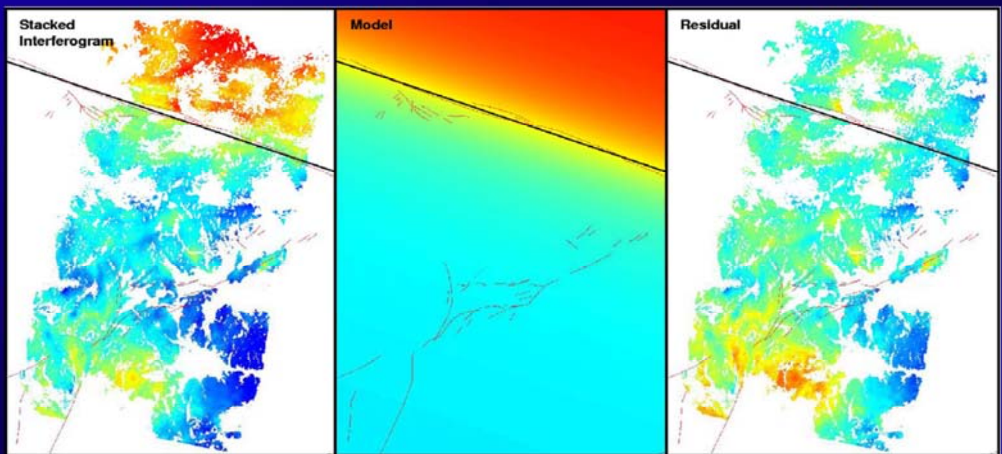

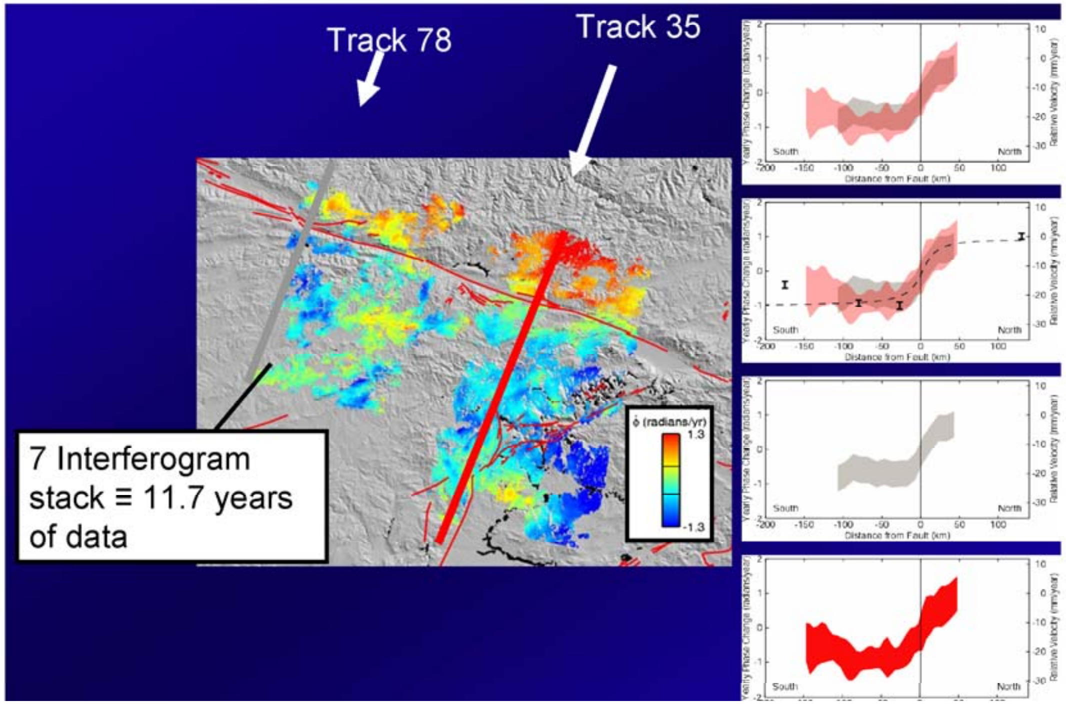

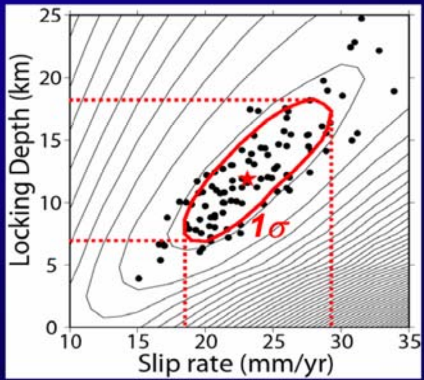

NAF Slip rate: 18-29 mm/yr

Locking Depth: 7-18 km

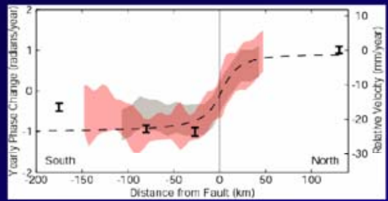

Triggered Slip on the Shahdad Thrust, Eastern Iran

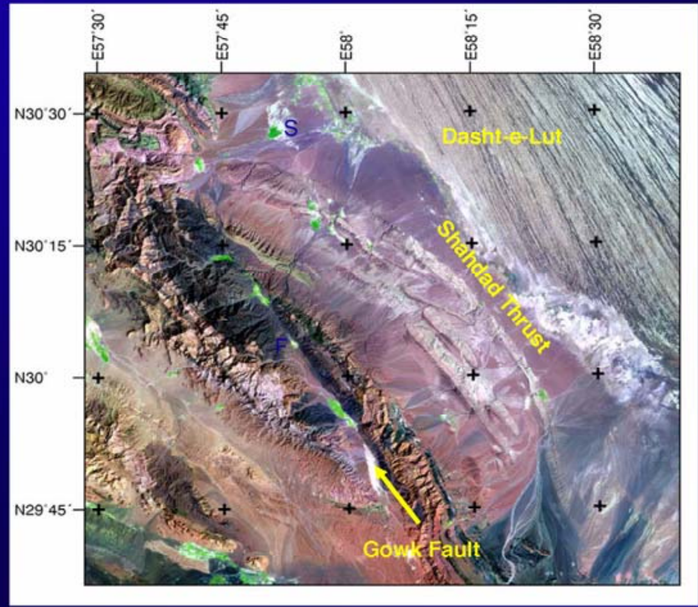

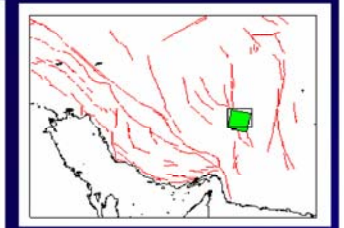

How wide is the shear zone at depth?

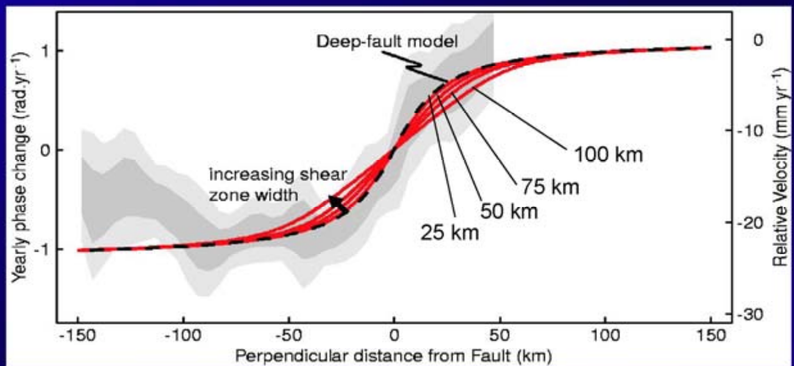

- For an 18 km elastic lid, a ~ 60 km wide shear zone at depth (π x lid thickness) cannot be distinguished from a deep, planar fault.

SAR Interferogram for the M_w 6.6 Fandoqa Earthquake, 14 March 1998, Eastern Iran

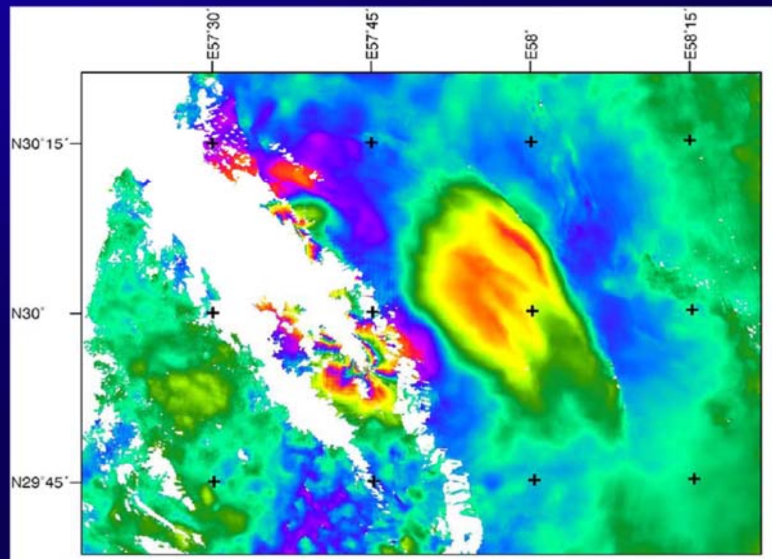

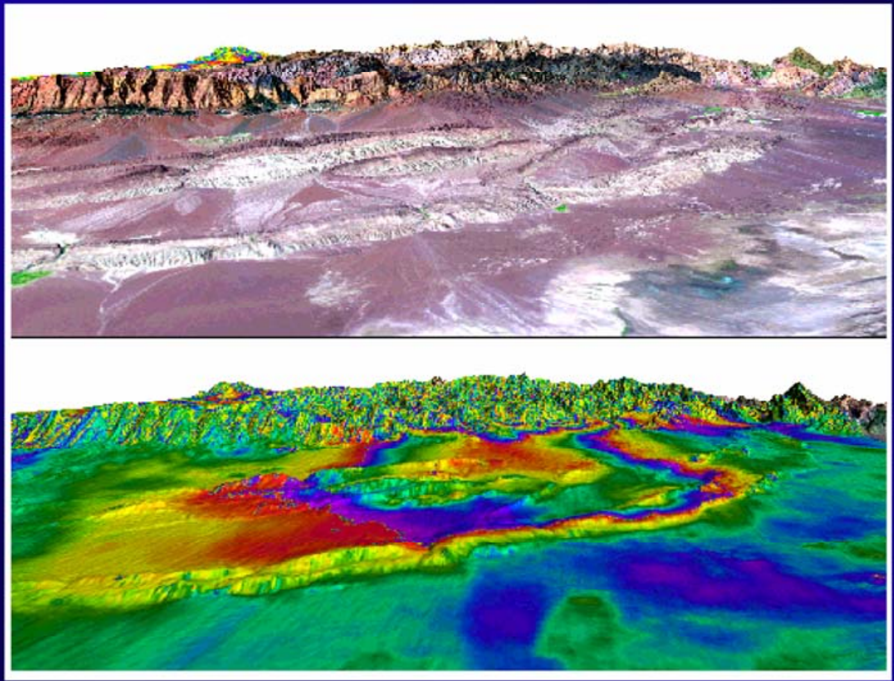

Postseismic Deformation

M_w ~ 7.1 Hector Mine Earthquake, October 16, 1999:

Rapid Postseismic Relaxation of upper mantle?

(Pollitz, Wicks & Thatcher, 2001)

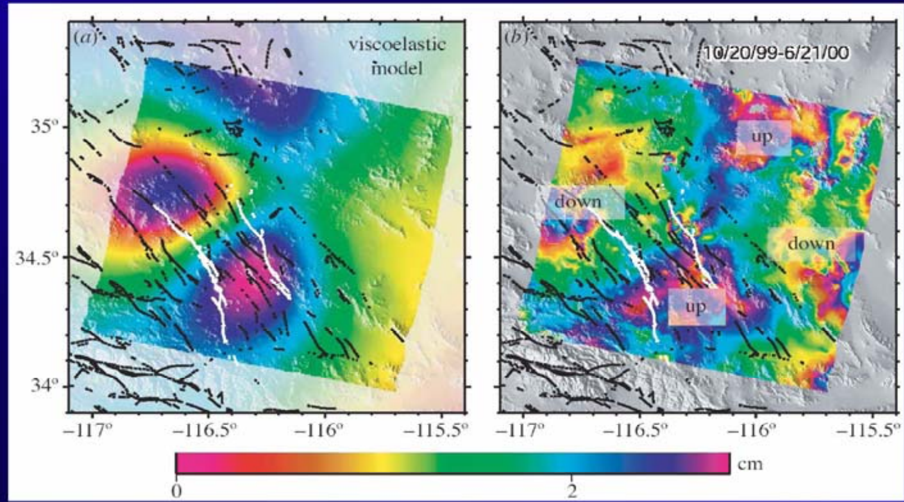

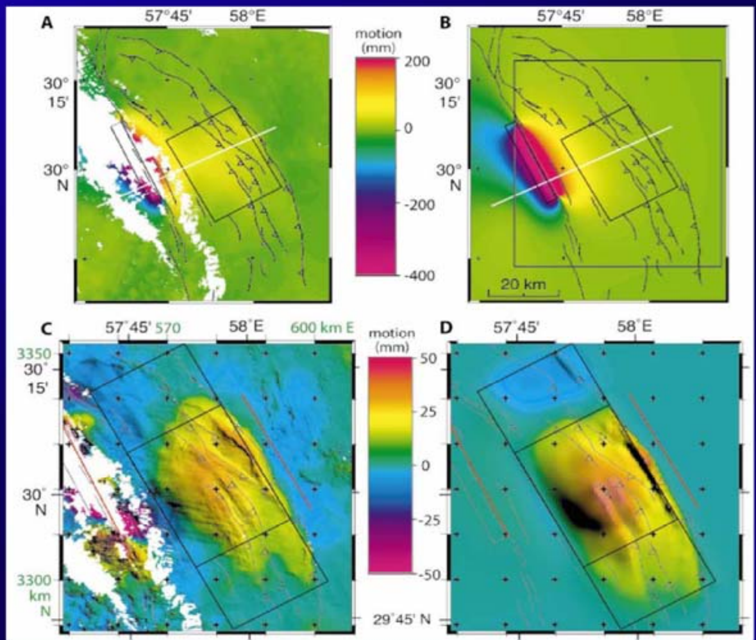

Fielding, E.J., T.J. Wright, J. Muller, B.E. Parsons, and R. Walker, *Geology*, 33(7), 577-580, 2004

Exploiting Envisat and the ERS archive

- Coseismic interferograms for upper-crustal earthquakes > M5.5 [< 8.0?].
- Interseismic deformation for faults with "reasonable" rates and "favourable" orientations.
- Postseismic transients for large earthquakes.
- Slow earthquakes, triggered aseismic slip and other unexpected phenomena.

If ground cover is suitable!

The practical class

Interpretation and modelling of

3 coseismic interferograms

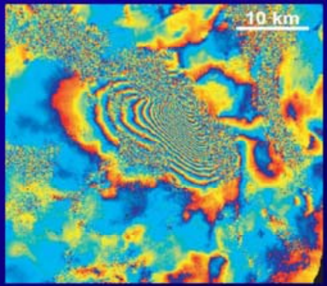

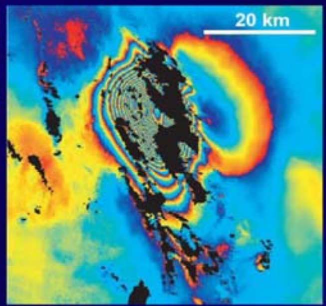

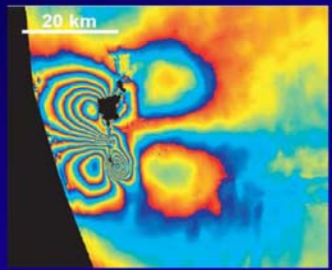

Reading List for InSAR and Earthquake-Cycle Deformation

Berberian, M., Baker, C., Fielding, E., Jackson, J., Parsons, B., Priestley, K., Qorashi, M., Talebian, M., Walker, R., and Wright, T. (2000). The 14 March 1998 Fandoqa earthquake (M_w 6.6) in Kerman province, S.E. Iran: re-rupture of the 1981 Sirch earthquake fault, triggering of slip on adjacent thrusts, and the active tectonics of the Gowk fault zone. *Geophys. J. Int.*, 146:371–398.

Bürgmann, R., Ayhan, M. E., Fielding, E. J., Wright, T. J., McClusky, S., Aktug, B., Demir, C., Lenk, O., and Türkezer, A. (2002). Deformation during the 12 November 1999, Düzce, Turkey earthquake, from GPS and InSAR data. *Bull. Seismol. Soc. Am.*, 92(4):161–171.

Bürgmann, R., Fielding, E., and Sukhatme, J. (1998). Slip along the Hayward fault, California estimated from space-based SAR interferometry. *Geology*, 26:559–562.

Bürgmann, R., Rosen, P., and Fielding, E. (2000a). Synthetic Aperture Radar interferometry to measure Earth's surface topography and its deformation. *Ann. Rev. Earth. Planet. Sci.*, 28:169–209.

Bürgmann, R., Schmidt, D., amd M. d'Alessio, R. N., Fielding, E., Manaker, D., McEvilly, T., and Murray, M. (2000b). Earthquake potential along the northern Hayward Fault, California. *Science*, 289:1,178–1,182.

Cattin, R., Briole, P., Lyon-Caen, H., and Pinettes, P. (1999). Effects of superficial layers on coseismic displacements for a dip-slip fault and geophysical implications. *Geophys. J. Int.*, 137:149–158.

Cervelli, P., Murray, M., Segall, P., Aoki, Y., and Kato, T. (2001). Estimating source parameters from deformation data, with an application to the March 1997 earthquake swarm off the Izu Peninsula, Japan. *J. Geophys. Res.*, 106:11,217–11,237.

Delouis, B., Giardini, D., Lundgren, P., and Salichon, J. (2002). Joint inversion of InSAR, teleseismic and strong motion data for the spatial and temporal distribution of earthquake slip: application to the 1999 Izmit mainshock. *Bull. Seismol. Soc. Am.*, 92(1):278–299.

Du, Y., Aydin, A., and Segall, P. (1992). Comparison of various inversion techniques as applied to the determination of a geophysical deformation model for the 1983 Borah Peak earthquake. *Bull. Seismol. Soc. Am.*, 82:1,840–1,866.

Feigl, K. L., Sarti, F., Vadon, H., McClusky, S., Ergintav, S., Bürgmann, R., Rigo, A., Massonnet, D., and Reilinger, R. (2002). Estimating slip distribution for the Izmit mainshock from coseismic GPS,ERS-1,RADARSAT, and spot measurements. *Bull. Seismol. Soc. Am.*, 92(1):138–160.

Feigl, K. L., Sergent, A., and Jacq, D. (1995). Estimation of an earthquake focal mechanism from a satellite radar interferogram; application to the December 4, 1992 Landers aftershock. *Geophys. Res. Lett.*, 22(9):1,037–1,040.

Fialko, Y., Simons, M., and Agnew, D. (2001). The complete (3-D) surface displacement field in the epicentral area of the 1999 M_w 7.1 Hector Mine earthquake, California, from space geodetic observations. *Geophys. Res. Lett.*, 28(16):3,063–3,066.

Fielding, E., Wright, T., Muller, J., Parsons, B., and Walker, R. (2004). Aseismic deformation of a fold-and-thrust belt imaged by SAR interferometry near Shahdad, SE Iran. *Geology*, 32(7):577–580, doi:10.1130/G20452.1.

Hernandez, B., Cotton, F., Campillo, M., and Massonnet, D. (1995). A comparison between short term (co-seismic) and long term (one year) slip for the Landers earthquake: Measurements from strong motion and SAR interferometry. *Geophys. Res. Lett.*, 22(18):2,517–2,520.

Jónsson, S., Zebker, H., Segall, P., and Amelung, F. (2002). Fault slip distribution of the 1999 Mw 7.1 Hector Mine earthquake, California, estimated from satellite radar and GPS measurements. *Bull. Seismol. Soc. Am.*, 92(4):1,377–1,389.

Lu, Z., Wright, T. J., and Wicks, C. (2003). Deformation of the 2002 Denali Fault earthquakes, Alaska, mapped by Radarsat-1 interferometry. *Eos*, 84(41):425, 430–431.

Massonnet, D., Feigl, K., Rossi, M., and Adragna, F. (1994). Radar interferometric mapping of deformation in the year after the Landers earthquake. *Nature*, 369:227–230.

Massonnet, D. and Feigl, K. L. (1995a). Discrimination of geophysical phenomena in satellite radar interferograms. *Geophys. Res. Lett.*, 22(12):1,537–1,540.

Massonnet, D. and Feigl, K. L. (1995b). Satellite radar interferometric map of the coseismic deformation field of the M = 6.1 Eureka Valley, California earthquake of May 17, 1993. *Geophys. Res. Lett.*, 22(12):1,541–1,544.

Massonnet, D. and Feigl, K. L. (1998). Radar interferometry and its application to changes in the earth's surface. *Rev. Geophys.*, 36(4):441–500.

Massonnet, D., Feigl, K. L., Vadon, H., and Rossi, M. (1996). Coseismic deformation field of the m = 6.7 Northridge, California earthquake of January 17, 1994 recorded by two radar satellites using interferometry. *Geophys. Res. Lett.*, 23(9):969–972.

Massonnet, D., Rossi, M., Carmona, C., Adragna, F., Peltzer, G., Feigl, K., and Rabaute, T. (1993). The displacement field of the Landers earthquake mapped by radar interferometry. *Nature*, 364:138–142.

Meyer, B., Armijo, R., de Chabalier, J., Delacourt, C., Ruegg, J., Acache, J., Briole, P., and Papanastassiou, D. (1996). The 1995 Grevena (Northern Greece) Earthquake: Fault model constrained with tectonic observations and SAR interferometry. *Geophys. Res. Lett.*, 23(19):2,677–2,680.

Okada, Y. (1985). Surface deformation due to shear and tensile faults in a half-space. *Bull. Seismol. Soc. Am.*, 75(4):1,135–1,154.

Ozawa, S., Murakami, M., Fujiwara, S., and Tobita, M. (1997). Synthetic aperture radar interferogram of the 1995 Kobe earthquake and its geodetic inversion. *Geophys. Res. Lett.*, 24(18):2,327–2,330.

Parsons, B., Wright, T. J., Andrews, J., Rowe, P., Jackson, J., Walker, R., Khatib, M., and Talebian, M. (2005). The 1994 Sefiadbeh earthquakes, eastern Iran: analysis of a growing fold. *Geophys. J. Int.*, In revision.

Peltzer, G., Crampé, F., Hensley, S., and Rosen, P. (2001). Transient strain accumulation and fault interaction in the Eastern California shear zone. *Geology*, 29(11):975–978.

Peltzer, G., Crampé, F., and King, G. (1999). Evidence of nonlinear elasticity of the crust from the Mw 7.6 Manyi (Tibet) earthquake. *Science*, 286:272–276.

Peltzer, G., Hudnut, K. W., and Feigl, K. L. (1994). Analysis of coseismic surface displacement gradients using radar interferometry: New insights into the Landers earthquake. *J. Geophys. Res.*, 99(B11):21,971–21,981.

Peltzer, G. and Rosen, P. (1995). Surface displacement of the 17 May 1993 Eureka Valley, California, earthquake observed by SAR interferometry. *Science*, 268:1,333–1,336.

Peltzer, G., Rosen, P., Rogez, F., and Hudnut, K. (1998). Poroelastic rebound along the Landers 1992 earthquake surface rupture. *J. Geophys. Res.*, 103(B12):30,131–30,145.

Pollitz, F., Peltzer, G., and Burgmann, R. (2000). Mobility of continental mantle: evidence from postseismic geodetic observations following the 1992 Landers earthquake. *J. Geophys. Res.*, 105(B4):8,035–8,054.

Pollitz, F., Wicks, C., and Thatcher, W. (2001). Mantle flow beneath a continental strike-slip fault: postseismic deformation after the 1999 Hector Mine earthquake. *Science*, 293:1,814–1,818.

Price, E. and Sandwell, D. (1998). Small-scale deformations associated with the 1992 Landers, California earthquake mapped by synthetic aperture radar interferometry phase gradients. *J. Geophys. Res.*, 103(11):27,001–27,016.

Pritchard, M. E., Simons, M., Rosen, P., Hensley, S., and Webb, F. (2002). Co-seismic slip from the 1995 July 30 Mw = 8.1 Antofagasta, Chile, earthquake as constrained by InSAR and GPS observations. *Geophys. J. Int.*, 150(2):362–376.

Reilinger, R., Ergintav, S., Bürgmann, R., McClusky, S., Lenk, O., Barka, A., Gurkan, O., Hearn, L., Feigl, K., Cakmak, R., Aktug, B., Ozener, H., and Töksoz, M. (2000). Coseismic and postseismic slip for the 17 August 1999, M=7.5, Izmit, Turkey earthquake. *Science*, 289:1,519–1,524.

Rosen, P., Hensley, S., Peltzer, G., and Simons, M. (2004). Updated Repeat Orbit Interferometry Package released. *Eos Trans. AGU*, 84(5):47.

Rosen, P., Werner, C., Fielding, E., Hensley, S., Buckley, S., and Vincent, P. (1998). Aseismic creep along the San Andreas Fault northwest of Parkfield, CA measured by radar interferometry. *J. Geophys. Res.*, 25(6):825–828.

Sandwell, D., Sichoix, L., Agnew, D., Bock, Y., and Minster, J.-B. (2000). Near real-time radar interferometry of the Mw 7.1 Hector Mine Earthquake. *Geophys. Res. Lett.*, 27(19):3,101–3,104.

Savage, J. and Burford, R. (1973). Geodetic determination of relative plate motion in Central California. *J. Geophys. Res.*, 78(5):832–845.

Talebian, M., Fielding, E., Funning, G., Ghorashi, M., Jackson, J., Nazari, H., Parsons, B., Priestley, K., Rosen, P., Walker, R., and Wright, T. (2004). The 2003 Bam (Iran) earthquake: rupture of a blind strike-slip fault. *Geophys. Res. Lett.*, 31(11):L11611, doi:10.1029/2004GL020058.

Wright, T., Parsons, B., England, P., and Fielding, E. (2004a). InSAR observations of low slip rates on the major faults of Western Tibet. *Science*, 305:236–239.

Wright, T., Parsons, B., and Lu, Z. (2004b). Toward mapping surface deformation in three dimensions using InSAR. *Geophys. Res. Lett.*, 31:L01607, doi:10.1029/2003GL018827.

Wright, T. J. (2000). *Crustal deformation in Turkey from Synthetic Aperture Radar Interferometry.* D.Phil. thesis, University of Oxford, Oxford, UK; ftp://ftp.earth.ox.ac.uk/pub/timw/thesis.tar.

Wright, T. J. (2002). Remote monitoring of the earthquake cycle using satellite radar interferometry. *Phil. Trans. R. Soc. Lond. A*, 360:2873–2888.

Wright, T. J., Fielding, E. J., and Parsons, B. E. (2001a). Triggered slip: observations of the 17 August 1999 Izmit (Turkey) earthquake using radar interferometry. *Geophys. Res. Lett.*, 28(6):1079–1082.

Wright, T. J., Lu, Z., and Wicks, C. (2003). Source model for the M_w 6.7, 23 October 2002, Nenana Mountain Earthquake (Alaska) from InSAR. *Geophys. Res. Lett.*, 30(18):1974, doi:10.1029/2003GL018014.

Wright, T. J., Lu, Z., and Wicks, C. (2005). Constraining the slip distribution and fault geometry of the M_w 7.9, 3 November 2002, Denali Fault Earthquake with InSAR and GPS. *Bull. Seismol. Soc. Am.*, In press.

Wright, T. J., Parsons, B., Jackson, J., Haynes, M., Fielding, E., England, P., and Clarke, P. (1999). Source parameters of the 1 October 1995 Dinar (Turkey) earthquake from SAR interferometry and seismic bodywave modelling. *Earth Planet. Sci. Lett.*, 172:23–37.

Wright, T. J., Parsons, B. E., and Fielding, E. J. (2001b). Measurement of interseismic strain accumulation across the North Anatolian Fault by satellite radar interferometry. *Geophys. Res. Lett.*, 28(10):2117–2120.

Zebker, H., Rosen, P., Goldstein, R., Gabriel, R., and Werner, C. (1994). On the derivation of coseismic displacement fields using differential radar interferometry: the Landers earthquake. *J. Geophys. Res.*, 99:19,617–19,634.